TIME-INHOMOGENEOUS QUANTUM MARKOV CHAINS

A Dissertation
Submitted to
the Temple University Graduate Board

---

in Partial Fulfillment
of the Requirements for the Degree of
DOCTOR OF PHILOSOPHY

---

by
Chia-Han Chou
August, 2020

Examining Committee Members:

Wei-Shih Yang, Advisory Chair, Mathematics
Gillian Queisser, Mathematics
Shiferaw Berhanu, Mathematics
Justin Shi, Computer and Information Science, Temple University

ABSTRACT

TIME-INHOMOGENEOUS QUANTUM MARKOV CHAINS

Chia-Han Chou

DOCTOR OF PHILOSOPHY

Temple University, August, 2020

Professor Wei-Shih Yang, Chair

In quantum computation theory, quantum Markov chains and quantum walks have been utilized by many quantum search algorithms which provide improved performance over their classical counterparts. More recently, due to the importance of the quantum decoherence phenomenon, decoherent quantum walks and their applications have been studied on a wide variety of structures. We study time-inhomogeneous quantum Markov chains with decoherence on finite spaces and discrete infinite spaces and their large scale equilibrium properties. In this thesis, we prove the convergence of decoherent time-inhomogeneous quantum Markov chain on finite state spaces, and a representation theorem for time-inhomogeneous quantum walk on discrete infinite state space. Additionally, the convergence of the distributions of the decoherent quantum walks are numerically estimated as an application of the representation theorem, and the convergence in distribution of the quantum

analogues of Bernoulli, uniform, arcsine and semicircle laws are statistically analyzed.

ACKNOWLEDGEMENTS

First and foremost, I want to thank my advisor, Professor Wei-Shih Yang, for the guidance and countless insights he provided, and for introducing me to the fascinating world of quantum computation. Additionally I would like to thank Professors Shiferaw Berhanu, Guillian Queisser, and Justin Shi for serving on my examining committee. Finally, I want to thank my friends and family for their ongoing support throughout my doctoral program.

Dedicated to my parents.

TABLE OF CONTENTS

LIST OF FIGURES

LIST OF TABLES

CHAPTER 1

INTRODUCTION

In order to develop more efficient algorithms for tackling a wide variety of problems in classical computer science, researchers started utilizing randomness techniques such as Ulam and von Nuemann's Markov Chain Monte Carlo (MCMC) method [14] in 1940s. This method was later refined and made well known as the Metropolis-Hastings algorithm [9] with applications in different areas. Even though Monte Carlos methods could sometimes return incorrect solutions with given probability, the key idea behind the methods was that the true solution can be approximated with high probability by repeating Monte Carlo simulations.

More recently, the notion of quantum computation has gained popularity, "qubit" takes a complex unit instead of "bit" the usual binary values of zero and one. To preserve a cohesive quantum system, the family of qubits com-

prising the memory of the computer go through unitary evolution, rather than the traditional system of gates in classical computation theory. The state of the quantum system can be observed, and collapsing the system to one unique state from a superposition of various state after the completion of each algorithm. The probability of observing any given state after observation is proportional to the absolute value squared of the amplitude of the system at that state. So, a false solution may in fact be observed which is similar to Monte-Carlo methods. However, if the algorithm is cleverly constructed, the correct solution is observed with significant likelihood.

Due to the quantum mechanical nature of quantum computation, new types of quantum algorithms have appeared. Moreover, these algorithms are more efficient than existing classical algorithms because the run times are better. For instance, both integer factorization and discrete logarithms undergo an exponential speedup using Shor's algorithm [16]. Not only an exponential improvement, Grover's search algorithm provides a quadratic speedup over any known classical search algorithm [8], and on a discrete space, Grover's algorithm is defined by discrete-time quantum walk, which is the natural extension of a Markov chain driven classical walk to the quantum setting.

On the other hand, if a quantum system were perfectly isolated, it would maintain coherence indefinitely, but it would be impossible to manipulate or investigate it. If it is not perfectly isolated, for example during a measurement,

coherence is shared with the environment and appears to be lost with time which is called quantum decoherence. This concept was first introduced by H. Zeh [18] in 1970, and then formulated mathematically for quantum walks by T. Brun [3]. For both coin and position space decoherent Hadamard walk, K. Zhang proved in [19] that with symmetric initial conditions, it has gaussian limiting distribution. More recently, the fact that the limiting distribution of the rescaled position discrete-time quantum random walks with general unitary operators subject to only coin space decoherence is a convex combination of normal distributions under certain conditions is proved by S. Fan, Z. Feng, S. Xiong and W. Yang [7]. The decoherent quantum analogues of Markov chains and random walks on a finite and discrete infinite space will be defined and elaborated in Chapter 2.

In fact, classical Markov chain limit theorems for the discrete time walks are well known and have had important applications in related areas [5] and [13]. However, the primary goal of this body of work is to examine the limiting behavior of the new model, discrete time-inhomogeneous quantum walk with decoherence on finite spaces and infinite discrete spaces, and generalize the results from the classical theorems to the quantum analogues. In Chapter 3, we obtain first-return properties of the time-inhomogeneous Markov chain with decoherence are derived rigorously in detail, and prove the convergence to equilibrium of the decoherent quantum Markov chains with time-inhomogeneous

unitary operators in general finite spaces using path integral formulas. Moreover, the equilibrium theory is illustrated by numerical simulations.

In Chapter 4, we study time-inhomogeneous quantum walk with decoherence on discrete infinite spaces, and prove a representation theorem for time-inhomogeneous quantum walk through path integral expressions. As the applications of the theorem, we introduce a new quantum algorithm with Monte Carlo technique to numerically approximate not only the classical symmetric Beta distributions and Bernoulli distributions, but also the limiting distributions of the decoherent time-inhomogeneous quantum walks.

Lastly, we introduce the quantum analogues of the classical distributions: arcsine, uniform, semicircle, and Bernoulli laws by considering the quantum walk in infinite discrete spaces without decoherence in Chapter 5. Even though it is extremely hard to study analytically the quantized classical distributions, we study their scaling limits and convergent rates, compare with their classical analogues, and statistically conclude that the quantum analogues of Bernoulli and Beta distributions under appropriate scaling exponents in this case are Bernoulli Laws.

CHAPTER 2

QUANTUM MARKOV CHAINS AND RANDOM WALKS

In classical probability, a random walk on $\mathbb{Z}$ is a Markov process described by a stochastic transition matrix T. On the other hand, for a quantum walk, instead of the transition matrix, the evolution of the system is described by a unitary operator U acting on a Hilbert space H. Several different models for quantum walks have been popularized. The two most commonly used are the coined walk of Aharonov et al [1] and the quantum markov chain of Szegedy [17]. Recently, S. Fan, Z. Feng, S. Xiong and W. Yang et al. [7] demonstrated that under certain conditions, the limiting distribution of the

rescaled position discrete-time decoherent quantum coined walks is a convex combination of normal distributions. All quantum walks elaborated here in this chapter are based on homogenuous coined Markov chains.

2.1 Decoherent quantum Markov chains

Let's consider the states $|1\rangle$ and $|2\rangle$ which represent the head and tail respectively when you flip a coin. Then, we suppose that they are orthonormal, and the coined Hilbert space H is defined by

$$H = span\{|1\rangle, |2\rangle\},$$

which means that any element in H can be written as linear combination of $|1\rangle$ and $|2\rangle$. And, we denote the inner product of the space by $\langle |i\rangle, |j\rangle\rangle := \langle i|j\rangle$, and $|i\rangle^* = \langle i|$ for $x = 1, 2$. Therefore, we have for instance,

$$\langle 1|1\rangle = 1, \text{ and } \langle 1|2\rangle = 0$$

On the other hand, let $U : H \to H$ be a unitary operator acting on the Hilbert space H itself. Recall that a unitary operator U satisfies the property that $UU^* = U^*U = I$ (where I denotes the identity operator, and U^* is the adjoint of U).

Now, in order to define a decoherent quantum Markov chain over the Hilbert space H, consider the decoherence parameter $p \in [0, 1]$, and define

for $i = 1, 2$

$$A_i = \sqrt{p} \cdot |i\rangle\langle i|,$$

and

$$A_0 = \sqrt{1-p} \cdot I$$

Note that $\{A_0, A_1, A_2\}$ has the property that $\sum_n {A_n}^* A_n = I$, and is called a measurement over the space H. This notion will be generally defined later in Section 2.2.1.

Definition 2.1 *Let $|x\rangle \in H$, and $\rho := |x\rangle\langle x|$, we define the time-homogeneous decoherent operator Φ such as*

$$\Phi(\rho) = \sum_{i=0}^{2} A_i U \rho U^* A_i^*$$

Now, suppose that $x \in \{1, 2\}$ is the initial position, and $\rho_0 = |x\rangle\langle x|$, and the n step time-homogeneous quantum Markov chain is defined as

$$\rho_n = \underbrace{\Phi \cdots \Phi}_{n \text{ times}}(\rho_0), \tag{2.1}$$

and, the probability of getting $y \in \{1, 2\}$ from the initial position $x \in \{1, 2\}$ after n steps is defined as the trace of $|y\rangle\langle y|\rho_n$, we denote it by

$$P_n(x, y) := Tr\Big(|y\rangle\langle y|\rho_n\Big). \tag{2.2}$$

Example 2.1 *Let U such as,*

$$U = \begin{bmatrix} \frac{1}{\sqrt{2}} & \frac{1}{\sqrt{2}} \\ \frac{1}{\sqrt{2}} & -\frac{1}{\sqrt{2}} \end{bmatrix} \tag{2.3}$$

Then the quantum Markov chain is called the Hadamard (fair coined) quantum Markov chain.

2.2 Quantum random walks

Now, we want to define the decoherent quantum random walk by generalizing the the idea from quantum Markov chain. First, We consider a pure quantum random walk on the 1-dimensional integer lattices $\mathbb{Z}$. The state space is a Hilbert space $H = H_p \otimes H_c$, where H_p denotes the position space, and H_c denotes the coin space, and $\otimes$ is the tensor product. The orthonormal basis of the position space are $\{|x\rangle, x \in Z\}$ and, the orthonormal basis of the coin space are $|1\rangle$ and $|2\rangle$. Tensor product of vector spaces and tensor operations are detailedly explained in [4].

Definition 2.2 *The standard shift operator $S_o : H \to H$ is a linear operator defined as follows*

$$S_o(|x\rangle \otimes |1\rangle) = |x+1\rangle \otimes |1\rangle$$

$$S_o(|x\rangle \otimes |2\rangle) = |x-1\rangle \otimes |2\rangle$$

Definition 2.3 *The flip-flop shift operator $S_f : H \to H$ is a linear operator defined as follows*

$$S_f(|x\rangle \otimes |1\rangle) = |x+1\rangle \otimes |2\rangle$$

$$S_f(|x\rangle \otimes |2\rangle) = |x-1\rangle \otimes |1\rangle$$

Note that we can also decompose the S_o and S_f as following

$$S_o = S^+ \otimes |1\rangle\langle 1| + S^- \otimes |2\rangle\langle 2|$$

$$S_f = S^+ \otimes |2\rangle\langle 1| + S^- \otimes |1\rangle\langle 2|$$

where $S^+, S^- : H_p \to H_p$ are linear operators defined by

$$S^+(|x\rangle) := |x+1\rangle \tag{2.4}$$

$$S^-(|x\rangle) := |x-1\rangle. \tag{2.5}$$

Let $F : H \to H$ be a unitary transformation on H defined by

$$F = \sum_{x \in Z} |x\rangle\langle x| \otimes C, \tag{2.6}$$

where $C : H_c \to H_c$ is a unitary operator. We can observe here that $|x\rangle\langle x|$ is the projection operator over the position space H_p.

Definition 2.4 *The evolution operator of quantum random walk is given by*

$$U = SF, \tag{2.7}$$

where $S = S_o$ for a standard quantum random walk, and $S = S_f$ for the flip-flop quantum random walk.

Let $|\psi_0\rangle \in H$. Then $|\psi_n\rangle = U^n|\psi_0\rangle = \underset{n \text{ times}}{U \cdots U}|\psi_0\rangle$ is called a quantum random walk with initial state $|\psi_0\rangle$. For convenience, we will use the short notation $|x^i\rangle = |x\rangle \otimes |i\rangle$.

The probability that at time step n, the quantum random walk is observed at state $|x^i\rangle$ is defined by

$$p_t(x^i) = |\langle x^i|\psi_t\rangle|^2,$$

and the probability that at time t, the quantum random walk is observed at state $|x\rangle$ is defined by

$$p_t(x) = \sum_{i=1}^{2} p_t(x^i) = \sum_{i=1}^{2} |\langle x^i|\psi_t\rangle|^2. \tag{2.8}$$

If the unitary operator does not depend on the position and time, the quantum walk is called homogeneous quantum walk.

Example 2.2 *Let $S = S_f$ and for all x,*

$$C = \begin{bmatrix} \frac{1}{\sqrt{2}} & \frac{1}{\sqrt{2}} \\ \frac{1}{\sqrt{2}} & -\frac{1}{\sqrt{2}} \end{bmatrix}$$

Then the quantum random walk is called the flip-flop Hadamard quantum random walk.

Example 2.3 *Let $S = S_o$ and for all x,*

$$C = \begin{bmatrix} \frac{1}{\sqrt{2}} & \frac{1}{\sqrt{2}} \\ \frac{1}{\sqrt{2}} & -\frac{1}{\sqrt{2}} \end{bmatrix}$$

Then the quantum random walk is called the standard Hadamard quantum random walk.

2.2.1 Decoherent walks

In physics, the quantum decoherence, in other words, lost of quantum coherence, is caused by environmental interactions. Mathematically, in quantum random walks, is defined by measurements.

Definition 2.5 *A set of operators* $\{A_n\}$ *on* H *is called a measurement if it satisfies*

$$\sum_n {A_n}^* A_n = I$$

Throughout this thesis, we also assume that the measurement is unital, i.e., it satisfies

$$\sum_n A_n A_n^* = I$$

Suppose before each unitary transformation, a measurement is performed. After the measurement, a density operator ρ on H is transformed by

$$\rho \to \rho' = \sum_n A_n \rho A_n^*.$$

Then after one step of the evolution and then under decoherence, the density operator becomes

$$\rho' = \sum_n A_n U \rho U^* A_n^* \tag{2.9}$$

Then the decoherent quantum random walk is defined as follows

Definition 2.6 *Let $\{A_n\}$ a measurement on the Hilbert space $H = H_p \otimes H_c$. Suppose we start from the state $|0\rangle \otimes |\Phi_0\rangle$, with $\Phi_0 \in \{1, 2\}$, then the initial state is given by the density operator $\rho_0 = |0\rangle\langle 0| \otimes |\Phi_0\rangle\langle\Phi_0|$, and the decoherent quantum walk $\{\rho_t\}_{t\in\mathbb{N}}$ with decoherence $\{A_n\}$ is defined by the following recursive relation:*

$$\rho_1 = \sum_n A_n U \rho_0 U^* A_n^*$$
$$\rho_t = \sum_n A_n U \rho_{t-1} U^* A_n^*$$

We can immediately deduce from the definition and obtain that for all $t = 1, 2, ...$

$$\rho_0 = |0\rangle\langle 0| \otimes |\Phi_0\rangle\langle\Phi_0| = (|0\rangle \otimes |\Phi_0\rangle)(\langle 0| \otimes \langle\Phi_0|),$$

$$\rho_t = \sum_{n_1,...,n_t} A_{n_t} U \cdots A_{n_1} U (|0\rangle \otimes |\Phi_0\rangle)(\langle 0| \otimes \langle\Phi_0|) U^* A_{n_1}^* \cdots U^* A_{n_t}^*$$

If we define the superoperator $\mathcal{L}$ to be an operator which maps $L(H)$ to $L(H)$ such that

$$\mathcal{L}B \equiv \sum_n A_n U B U^* A_n^*, \ \forall B \in L(H), \tag{2.10}$$

then

$$\rho_t = \mathcal{L}^t \rho_0. \tag{2.11}$$

For decoherent quantum random walk with decoherence $\{A_n\}$, the probability of reaching a point x at time t is defined by

$$\begin{aligned} p_d(x,t) &= Tr[(|x><x| \otimes I_c)\rho_t] \\ &= Tr[(|x><x| \otimes I_c)\mathcal{L}^t \rho_0], \end{aligned} \tag{2.12}$$

where $Tr(\cdot)$ denotes the trace operator.

Interpreting the definitions in physics, for the measurements we defined in section 2.1, we perform a measurement at $\{|i\rangle\langle i|\}$ with probability p and no measurement with probability $q = 1 - p$ at each time step n. If at the measurement step, the outcome is $|i\rangle$, then the system is reset to $|i\rangle$. On the other hand, we can also easily observe that if $p = 1$, measurement at each time step with probability 1, ρ_n will represent the classical Markov chain or random walk. Intuitively, ρ_n will be the pure quantum Markov chain or quantum walk if $p = 0$.

The following examples show different decohorent quantum walks with different types of measurements $\{A_n\}_{n\in\mathbb{N}}$

Example 2.4 *Let* $0 \leq p \leq 1$, $A_0 = \sqrt{1-p}I_H$, *and* $A_{xi} = \sqrt{p}(|x\rangle \otimes |i\rangle)(\langle x| \otimes \langle i|)$. *Then* $\{A_0, A_{xi}; x \in Z^1, i = 1, 2\}$ *is a measurement on* H. *When* $0 < p \leq 1$, ρ_t *is called a totally (coin-space) decoherent quantum random walk.*

Example 2.5 *Let* $0 \leq p \leq 1$, $A_\emptyset = \sqrt{1-p}I_H$, *and* $A_x = \sqrt{p}|x\rangle\langle x| \otimes I_c$. *Then* $\{A_\emptyset, A_x; x \in Z^1\}$ *is a measurement on* H, *and when* $0 < p \leq 1$, ρ_t *is called a position space decoherent quantum random walk.*

Example 2.6 *Let* $0 \leq p \leq 1$, $A_0 = \sqrt{1-p}I_H$, *and* $A_i = \sqrt{p}I_p \otimes |i\rangle\langle i|$. *Then* $\{A_0, A_i; i = 1, 2\}$ *is a measurement on* H, *and when* $0 < p \leq 1$, ρ_t *is called a coin space decoherent quantum random walk.*

Considering the general measurement $\{A_n\}$ and the homogeneous unitary operator C, one of the recent and important achievements is that in [7], S. Fan, Z. Feng , S. Xiong and W. Yang proved that under some conditions of the superoperator $\mathcal{L}$, the rescaled probability mass function on $\frac{\mathbb{Z}}{\sqrt{t}}$ by

$$\hat{p}(x,t) \equiv p_d(\sqrt{t}x,t),\ x \in \frac{\mathbb{Z}}{\sqrt{t}}$$

converges in distribution to a continuous convex combination of normal distributions. Later in Chapters 3 and 4, we will mainly discuss the large scale behavior of quantum Markov chains and quantum walks with the time-inhomogenuous unitary operator from Example 4.3 and the coin space decoherence measurement from Example 2.6.

CHAPTER 3

TIME-INHOMOGENEOUS QUANTUM MARKOV CHAINS

In classical probability theory, a discrete-time Markov chain on a finite state space is a sequence of random variables $\{X_n\}_{n\in\mathbb{N}}$ on a finite state space with the property that the conditional probability distribution of future states of the process depends only upon the present state, not on the sequence of events that preceded it, in other words, the future outcomes depends only on the present result, not the past ones. We also call this phenomenon Markov property. With the decoherence parameter $p \in (0, 1]$, classical Markov chains on finite state spaces can naturally extend to decoherent quantum Markov

chains as we defined in section 2.1.

In this chapter, instead of homogeneous unitary operators U, let's first consider $U_n : H \to H$, unitary defined by

$$U_n = \begin{bmatrix} \sqrt{1-\frac{\lambda}{n^\zeta}} & \sqrt{\frac{\lambda}{n^\zeta}} \\ \sqrt{\frac{\lambda}{n^\zeta}} & -\sqrt{1-\frac{\lambda}{n^\zeta}} \end{bmatrix},$$

time inhomogeneous unitary operators, where λ and ζ are non negative real numbers. And we can define the decoherent time-inhomogeneous quantum Markov chain by extending the definitions from Section 2.1 with

$$\Phi_n(\rho) = \sum_{i=0}^{2} A_i U_n \rho {U_n}^* A_i^* \tag{3.1}$$

with $A_0 = \sqrt{1-p}\cdot I$, and $A_i = \sqrt{p}\cdot|i\rangle\langle i|$, for $p \in [0,1]$, and $i = 1, 2$. Similarly

$$\rho_n = \Phi_n \cdots \Phi_1(\rho_0), \tag{3.2}$$

Therefore, the probability of getting $y \in \{1,2\}$ from $x \in \{1,2\}$ at time n is defined as

$$P_n(x,y) := Tr\Big(|y\rangle\langle y|\rho_n\Big). \tag{3.3}$$

Note that we can easily obtain the homogeneous case from this setting by letting $\zeta = 0$. For example, if $\zeta = 0$ and $\lambda = \frac{1}{2}$, we have the fair coined quantum Markov chain from Example 2.1.

3.1 Path integral formula and basic properties

Let's start by proving some basic properties before we go to the equilibrium convergence theorem. First, if we suppose that the quantum Markov chain we defined is completely decoherent, $p = 1$, we have

$$\Phi_n(\rho) = \sum_{i=1}^{2} A_i U_n \rho U_n^* A_i^*$$

and

$$P_n(i,j) = Tr\Big(|j\rangle\langle j|\Phi_n|i\rangle\langle i|\Big)$$

where ρ is any 2 by 2 density matrix, and $i, j = 1, 2$. Using the fact that $|k\rangle, k = 1, 2, ...$ are orthonormal basis, we obtain

$$\begin{aligned} P_n(i,j) &= \sum_{k=1}^{2} Tr\Big(|j\rangle\langle j|k\rangle\langle k|U_n|i\rangle\langle i|U_n^*|k\rangle\langle k|\Big) \\ &= \sum_{k=1}^{2} Tr\Big(\langle j|k\rangle\langle k|U_n|i\rangle\langle i|U_n^*|k\rangle\langle k|j\rangle)\Big) \\ &= Tr\Big(\langle j|U_n|i\rangle\langle i|U_n^*|j\rangle\Big) = U_n(j,i)U_n^*(i,j) = |U_n(j,i)|^2 \end{aligned}$$

If $\zeta = 0$ and $p = 1$, then it reduces to time-homogeneous Markov chain and it is well known that $\rho_n \to \rho_\infty$ when $n \to \infty$ by the Ergodic Theorem for finite-state Markov chains. Our focus now will be for the case of $\zeta > 0$ or $0 < p < 1$.

By Kolomogorov 0-1 law, for $0 < p \leq 1$, there exists an infinite sequence of measurement when $t \to \infty$. Therefore, if $X_1, X_2, ...$ are the outcome of the

measurements, then $\{X_n\}_{n=1}^{\infty}$ is a Markov chain (time-inhomogeneous Markov chain).

Definition 3.1 *Let $\{T_n\}_{n=1}^{\infty}$ be i.i.d. geometric random variables with mean $\frac{1}{p}$, and let $\sigma_0 = 0$ and $\sigma_n = T_1 + \cdots + T_n$, and define*

$$Q_n(i,j) := E\Big[\big|\langle j|U_{\sigma_{n-1}+T_n}\cdots U_{\sigma_{n-1}+1}|i\rangle\big|^2\Big] \tag{3.4}$$

Proposition 3.1 *Let $\{T_n\}_{n=1}^{\infty}$ be i.i.d. geometric random variables with mean $\frac{1}{p}$, and let $\sigma_0 = 0$ and $\sigma_n = T_1 + \cdots + T_n$. Then*

(a) $P\big(X_1 = i_1, X_2 = i_2, ..., X_n = i_n\big) = E\Big[\big|\langle i_n|U_{\sigma_n}\cdots U_{\sigma_{n-1}+1}|i_{n-1}\rangle\big|^2\cdots$

$$\cdots\big|\langle i_1|U_{\sigma_1}\cdots U_1|i\rangle\big|^2\Big]$$

(b) $P\big(X_n = i_n|X_1 = i_1, X_2 = i_2, ..., X_{n-1} = i_{n-1}\big) = P\big(X_n = i_n|X_{n-1} = i_{n-1}\big)$

$$= Q\big(i_{n-1}, i_n\big)$$

Proof of 3.1: Let $\Phi_k(\rho) = \sum_{i=0}^{2} A_i U_k \rho U_k^* A_i$, $\rho \in \mathcal{E}$, where $\mathcal{E}$ =the set of all density operators on H. The quantum operation of the partially decoherent quantum process at step k is given by Φ_k.

Suppose that the initial state is $\rho_0 = |i\rangle\langle i|$. Then the state at time t is

$$\rho_t = \Phi_t \cdots \Phi_1(\rho_0)$$

The probability at time t, the system is found at state $|j\rangle$ is given by

$$Tr(|j\rangle\langle j|\rho_t) = Tr\Big(\langle j|\sum_{j_t=0}^{2}\cdots\sum_{j_1=0}^{2} A_{j_t}U_t\cdots A_{j_2}U_2A_{j_1}U_1|i\rangle\langle i|U_1^*A_{j_1}^*\cdots U_t^*A_{j_t}^*|j\rangle\Big)$$

$$= \sum_{j_t=0}^{2}\cdots\sum_{j_1=0}^{2} Tr\Big(\langle j|A_{j_t}U_t\cdots A_{j_2}U_2A_{j_1}U_1|i\rangle\langle i|U_1^*A_{j_1}^*\cdots U_t^*A_{j_t}^*|j\rangle\Big)$$

$$= \sum_{j_t,\ldots,j_1=0}^{2} \big|\langle j|A_{j_t}U_t\cdots A_{j_2}U_2A_{j_1}U_1|i\rangle\big|^2$$

In each term of above sum, let $0 < \sigma_1 < \sigma_2 < ... < \sigma_n \leq t$ be the times that $j_{\sigma_k} = 1$ or 2, and $j_s = 0$ for all $s \neq \sigma_1, ..., \sigma_n$. $0 < \sigma_1 < \sigma_2 < ... < \sigma_n$ are called decoherence time, and we put $i_k = j_{\sigma_k}$. So, the sum can be written as,

$$Tr(|j\rangle\langle j|\rho_t) = \sum_{n=0}^{\infty}\sum_{0=\sigma_0<\ldots<\sigma_n\leq t} p^n q^{t-n}\sum_{i_n=1}^{2}\cdots\sum_{i_1=1}^{2}\big|\langle j|U_t\cdots U_{\sigma_n+1}|i_n\rangle\big|^2\cdot$$

$$\cdot\big|\langle i_n|U_{\sigma_n}\cdots U_{\sigma_{n-1}+1}|i_{n-1}\rangle\big|^2\cdots\big|\langle i_1|U_{\sigma_1}\cdots U_1|i\rangle\big|^2 \tag{3.5}$$

Now, let's proof part (a) of the proposition,

$$P\big(X_1 = i_1, ..., X_n = i_n\big) = \sum_{t=1}^{\infty} P\big(X_1 = i_1, ..., X_n = i_n, \sigma_n = t\big)$$

$$= \sum_{t=1}^{\infty}\sum_{0<\sigma_1<\cdots<\sigma_n=t} P_{\sigma_1,\ldots,\sigma_n,t}\big(i_1, ..., i_n, j\big) \text{ where } t = \sigma_n \text{ and } j = i_n$$

$$= \sum_{0<\sigma_1<\cdots<\sigma_n<\infty} p^n q^{\sigma_n - n}\big|\langle i_n|U_{\sigma_n}\cdots U_{\sigma_{n-1}+1}|i_{n-1}\rangle\big|^2\cdots\big|\langle i_1|U_{\sigma_1}\cdots U_1|i\rangle\big|^2$$

$$= E\Big[\big|\langle i_n|U_{\sigma_n}\cdots U_{\sigma_{n-1}+1}|i_{n-1}\rangle\big|^2\cdots\big|\langle i_1|U_{\sigma_1}\cdots U_1|i\rangle\big|^2\Big]$$

To prove (b), note that from (a), by independence of $\{T_n\}_{n=1}^{\infty}$

$$P\big(X_1 = i_1, X_2 = i_2, ..., X_n = i_n\big) = Q_1(i, i_1)\cdots Q_1(i_{n-1}, i_n)$$

Then,

$$P\big(X_n = i_n | X_1 = i_1, ..., X_{n-1} = i_{n-1}\big) = \frac{P\big(X_1 = i_1, ..., X_{n-1} = i_{n-1}, X_n = i_n\big)}{P\big(X_1 = i_1, ..., X_{n-1} = i_{n-1}\big)}$$

$$= Q_n(i_{n-1}, i_n)$$

We can also note that

$$P\big(X_n = i_n | X_{n-1} = i_{n-1}\big) = \frac{P\big(X_n = i_n, X_{n-1} = i_{n-1}\big)}{P\big(X_{n-1} = i_{n-1}\big)}$$

$$= \frac{\sum_{i_1,...,i_{n-2}=1}^{2} Q_1(i, i_1) \cdots Q_1(i_{n-2}, i_{n-1}) Q_n(i_{n-1}, i_n)}{\sum_{i_1,...,i_{n-2}=1}^{2} Q_1(i, i_1) \cdots Q_1(i_{n-2}, i_{n-1})} = Q_n(i_{n-1}, i_n)$$

□

Remarks:

(a) It follows from Proposition 3.1 (b) that $X_1, X_2, ...$ is a time inhomogeneous Markov chain with transition probability

$$P\big(X_n = j | X_{n-1} = i\big) = Q_n(i, j), \ 1 \leq i, j \leq 2,$$

and this is illustrated in the following diagram

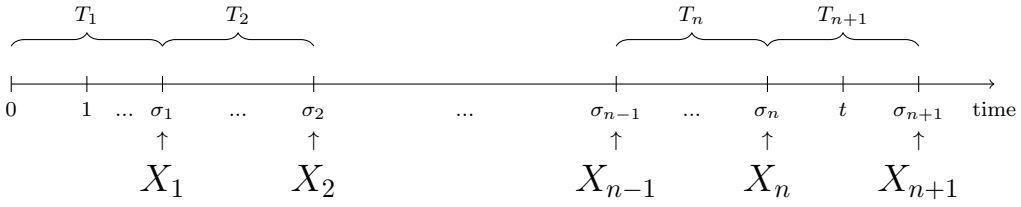

(b) This proposition gives a probabilistic interpretation of decoherence time $0 < \sigma_0 < \sigma_1 < ... < \sigma_n < ...$ as a sequence of arrival times of independence Bernoulli trials with success probability p, and $\{X_n\}_{n=1}^{\infty}$ can be viewed as discrete version of a compound Poisson process.

(c) For $\sigma_n \leq t$, and from Equation (3.5), we obtain an expression for the probability that the system is found at state j with exact decoherent time $\sigma_1, ...\sigma_n$ and outcomes $i_1, i_2, ..., i_n$.

Definition 3.2 (Path integral formula) *The probability that the system is found at state j with exact decoherent time $\sigma_1, ..., \sigma_n$ and outcomes $i_1, i_2, ..., i_n$, in this case $X_1 = i_1, ...X_n = i_n$ if $\sigma_n \leq t$, for the decoherent quantum random walk for $0 < p \leq 1$ can be written as the path integral formula:*

$$P_{\sigma_1,\sigma_2,...,\sigma_n,t}\big(i_1, i_2, ..., i_n, j\big) := p^n q^{t-n} \big|\langle j|U_t \cdots U_{\sigma_n+1}|i_n\rangle\big|^2 \cdots \big|\langle i_1|U_{\sigma_1} \cdots U_1|i\rangle\big|^2$$

The path integral formula defined in Definition 3.2 is not only very intuitive expression to understand the probability of an specific path from the initial state, but also very useful for generating numerical simulations. We will discuss the simulation applications in Section 3.4.

3.2 Convergence to equilibrium

Before we prove the convergence, let's first observe that Q_n defined in Definition 3.1 is doubly stochastic which will be useful later in the proof.

Proposition 3.2 *Q_n is doubly stochastic for all $n \in \mathbb{N}$.*

Proof of 3.2: Note that a matrix $A = (a_{ij})$ is doubly stochastic if

$$\sum_i a_{ij} = 1 \quad \text{for all } j$$

and

$$\sum_j a_{ij} = 1 \ \text{ for all } i$$

So, we have for all $j = 1, 2$,

$$\sum_{i=1}^{2} Q_n(i,j) = \sum_{i=1}^{2} E\Big[\langle j|U_{\sigma_{n-1}+T_n}\cdots U_{\sigma_{n-1}+1}|i\rangle\langle i|U^*_{\sigma_{n-1}+1}\cdots U^*_{\sigma_{n-1}+T_n}|j\rangle\Big]$$

$$= E\Big[\sum_{i=1}^{2} Tr\big[|j\rangle\langle j|U_{\sigma_{n-1}+T_n}\cdots U_{\sigma_{n-1}+1}|i\rangle\langle i|U^*_{\sigma_{n-1}+1}\cdots U^*_{\sigma_{n-1}+T_n}\big]\Big]$$

$$= E\big[Tr\big(|j\rangle\langle j|\big)\big] = 1$$

And also, $\sum_{j=1}^{2} Q_n(i,j) = 1$ for all $i = 1, 2$ by similar argument.

□

Finally, we have the equilibrium property

Proposition 3.3 *If* $0 < \zeta \leq 1$, *then*

$$Q_1Q_2Q_3\cdots Q_n \to \Pi = \begin{bmatrix} 1/2 & 1/2 \\ \\ 1/2 & 1/2 \end{bmatrix},$$

as $n \to \infty$, *for all* $0 < p \leq 1$.

Proof of 3.3 : Let's consider first the homogeneous case, and let $\delta > 0$ such that $Q \geq \delta\Pi$. Note that for any $\alpha > 0$, we can write

$$Q = \alpha\Big(\frac{Q - \delta\Pi}{\alpha}\Big) + \delta\Pi = \alpha\tilde{Q} + \delta\Pi$$

where $\tilde{Q} = \frac{Q-\delta\Pi}{\alpha}$ is a stochastic matrix, and then

$$Q^n = \big(\alpha\tilde{Q} + \delta\Pi\big)^n$$

$$= \sum_{k=0}^{n} \alpha^{n-k}\delta^{k}\Big[\binom{n}{k} \text{ terms of different combinations of n-k } \tilde{Q}\text{'s and k } \Pi\text{'s}\Big]$$

Now, take $\alpha = \sum_{j} \big(Q - \delta\Pi\big)(i,j) = 1 - \delta$ and use the fact that Q is doubly stochastic, we have the following,

1. $\alpha + \delta = 1$ by construction.

2. $\Pi \cdot \Pi = \Pi$.

3. $\tilde{Q} \cdot \Pi = \dfrac{Q - \delta\Pi}{\alpha}\Pi = \dfrac{Q\Pi - \delta\Pi^2}{\alpha} = \dfrac{\Pi - \delta\Pi}{\alpha} = \dfrac{1-\delta}{\alpha}\Pi = \Pi$

4. Similarly, we have $\Pi \cdot \tilde{Q} = \Pi$

5. $\tilde{Q}$ is doubly stochastic.

Now, since $\alpha < 1$ we have

$$Q^n = \alpha^n \tilde{Q}^n + \sum_{k=1}^{n} \alpha^{n-k}\delta^{k}\binom{n}{k}\Pi = \alpha^n\tilde{Q}^n + \big[(\alpha+\delta)^n - \alpha^n\big]\Pi$$

$$= \alpha^n\tilde{Q}^n + (1-\alpha^n)\Pi \to \Pi \text{ as } n \to \infty$$

For the inhomogeneous case, X_1, X_2, X_3... is a Markov chain, we note that by independence and properties of conditional probability

$$Q_n(i,j) = P(X_n = j | X_{n-1} = i)$$

$$= \sum_{s=1}^{\infty}\sum_{t=1}^{\infty} P\big(X_n = j | X_{n-1} = i, \sigma_{n-1} = s, T_n = t\big) \cdot P\big(\sigma_{n-1} = s, T_n = t | X_{n-1} = i\big)$$

$$= \sum_{s=1}^{\infty}\sum_{t=1}^{\infty} \Big|\langle j|U_{s+t}\cdots U_{s+1}|i\rangle\Big|^2 \cdot P\big(T_n = t | \sigma_{n-1} = s\big) \cdot P\big(\sigma_{n-1} = s\big)$$

$$= \sum_{s=1}^{\infty}\sum_{t=1}^{\infty}\Big|\langle j|U_{s+t}\cdots U_{s+1}|i\rangle\Big|^2 \cdot P\big(T_n = t\big)\cdot P\big(\sigma_{n-1}=s\big)$$

Note that if we consider only the term $t=1$, and using the fact that $P\big(T_n = t/\sigma_{n-1}=s\big) = q^{t-1}p$, we have

$$Q_n(i,j) \geq \sum_{s=1}^{\infty}\Big|\langle j|U_{s+1}|i\rangle\Big|^2 \cdot p\cdot P\big(\sigma_{n-1}=s\big)$$

$$= p\sum_{s=1}^{\infty}\Big|\langle j|U_{s+1}|i\rangle\Big|^2 \cdot P\big(\sigma_{n-1}=s\big) \geq p\sum_{s=1}^{\infty}\frac{\lambda}{(s+1)^{\zeta}}\cdot P\big(\sigma_{n-1}=s\big)$$

$$= p\lambda\cdot E\Big[\frac{1}{(\sigma_{n-1}+1)^{\zeta}}\Big] \geq \delta_n\cdot\Pi$$

Where $\delta_n = 2p\lambda\cdot E\Big[\frac{1}{(\sigma_{n-1}+1)^{\zeta}}\Big]$.Therefore,

$$Q_n = \alpha_n\Big(\frac{Q_n-\delta_n\Pi}{\alpha_n}\Big)+\delta_n\Pi = \alpha_n\tilde{Q}_n+\delta_n\Pi$$

Since $\alpha_n = 1-\delta_n$ and $\tilde{Q}_n$ is stochastic.

$$Q_1Q_2\cdots Q_n = \prod_{k=1}^{n}\big[\alpha_n\tilde{Q}_n+\delta_n\Pi\big] = \prod_{k=1}^{n}\alpha_k\tilde{Q}_k+\big(1-\prod_{k=1}^{n}\alpha_k\big)\Pi$$

The last equality can be proved by induction, if n=2

$$\big[\alpha_1\tilde{Q}_1+(1-\alpha_1)\Pi\big]\cdot\big[\alpha_2\tilde{Q}_2+(1-\alpha_2)\Pi\big]$$

$$= \alpha_1\alpha_2\tilde{Q}_1\tilde{Q}_2+(1-\alpha_1)\alpha_2\Pi\tilde{Q}_2+\alpha_1(1-\alpha_2)\tilde{Q}_1\Pi+(1-\alpha_1)(1-\alpha_2)\Pi^2$$

$$= \alpha_1\alpha_2\tilde{Q}_1\tilde{Q}_2+\Pi-\alpha_1\alpha_2\Pi+\alpha_1\Pi-\alpha_1\alpha_2\Pi-\Pi+\alpha_1\alpha_2\Pi+\Pi-\alpha_1\Pi =$$

$$\alpha_1\alpha_2\tilde{Q}_1\tilde{Q}_2+(1-\alpha_1\alpha_2)\Pi$$

And now, let's assume that the formula is true for n, and prove it for $n+1$,

$$\prod_{k=1}^{n+1}\left[\alpha_n\tilde{Q}_n+\delta_n\Pi\right]=\Big[\prod_{k=1}^{n}\alpha_k\tilde{Q}_k+\big(1-\prod_{k=1}^{n}\alpha_k\big)\Pi\Big]\Big[\alpha_{n+1}\tilde{Q}_{n+1}+(1-\alpha_{n+1})\Pi\Big]$$

$$=\prod_{k=1}^{n+1}\alpha_k\tilde{Q}_k+\prod_{k=1}^{n}\alpha_k(1-\alpha_{n+1})\Pi+\big(1-\prod_{k=1}^{n}\alpha_k\big)\alpha_{n+1}\Pi+\big(1-\prod_{k=1}^{n}\alpha_k\big)(1-\alpha_{n+1})\Pi$$

$$=\prod_{k=1}^{n+1}\alpha_k\tilde{Q}_k+\prod_{k=1}^{n}\alpha_k\Pi-\prod_{k=1}^{n+1}\alpha_k\Pi+\alpha_{n+1}\Pi-\prod_{k=1}^{n+1}\alpha_k\Pi+\Pi-\alpha_{n+1}\Pi-\prod_{k=1}^{n}\alpha_k\Pi+\prod_{k=1}^{n+1}\alpha_k\Pi$$

$$=\prod_{k=1}^{n+1}\alpha_k\tilde{Q}_k-\big(1-\prod_{k=1}^{n+1}\alpha_k\big)\Pi$$

We observe that if $\prod_{k=1}^{\infty}\alpha_k=0$, $Q_1Q_2\cdots Q_n\to\Pi$, and we have obtained the conclusion.

To check this, note that

$$\prod_{k=1}^{n}\alpha_k=\prod_{k=1}^{n}(1-\delta_k)=\prod_{k=1}^{n}\Big[1-2p\lambda E\big[\frac{1}{(\sigma_{k-1}+1)^{\zeta}}\big]\Big]$$

$$=e^{\sum_{k=1}^{n}\ln\left[1-2p\lambda E\left[\frac{1}{(\sigma_{k-1}+1)^{\zeta}}\right]\right]}\leq e^{-\sum_{k=1}^{n}2p\lambda E\left[\frac{1}{(\sigma_{k-1}+1)^{\zeta}}\right]}$$

since $\ln(1-x)\leq -x$ for $0<x<1$.

Observe that each $T_k\geq 1$, so we have, $\frac{T_1+\ldots T_{k-1}+1}{k-1}\geq 1+\frac{1}{k-1}$ for all k , and this implies

$$\frac{1}{\frac{T_1+\ldots+T_{k-1}+1}{k-1}}\leq\frac{1}{1+\frac{1}{k-1}}\leq 1$$

Which means that by the Bounded Convergence Theorem,

$$E\big[\frac{1}{(\sigma_{k-1}+1)^{\zeta}}\big]$$

$$= E\Big[\frac{1}{\big(\frac{T_1+T_2+\cdots+T_{k-1}+1}{k-1}\big)^{\zeta}}\Big]\frac{1}{(k-1)^{\zeta}} \to \frac{1}{(E(T_1))^{\zeta}}\frac{1}{(k-1)^{\zeta}} = \frac{p^{\zeta}}{(k-1)^{\zeta}}$$

as $k \to \infty$

Therefore,

$$\prod_{k=1}^{n}\alpha_k \leq e^{-\sum_{k=1}^{n} 2p\lambda E\left[\frac{1}{(\sigma_{k-1}+1)^{\zeta}}\right]} \leq \exp\Big(-\sum_{k=1}^{n}\frac{p^{\zeta}}{(k-1)^{\zeta}}\Big[\frac{E\left[\frac{1}{(\sigma_{k-1}+1)^{\zeta}}\right]}{\frac{p^{\zeta}}{(k-1)^{\zeta}}}\Big]\Big)$$

Now, since $\dfrac{E\left[\frac{1}{(\sigma_{k-1}+1)^{\zeta}}\right]}{\frac{p^{\zeta}}{(k-1)^{\zeta}}} \to 1$ as $k \to \infty$, we have that $\prod_{k=1}^{n}\alpha_k \to 0$ if $\zeta \leq 1$
And, we conclude that, $Q_1 \cdots Q_n \to \Pi$ for all $0 \leq \zeta \leq 1$ and $0 < p \leq 1$. □

Note that for the special homogeneous case $\zeta = 0$, the result is already known, and it was proved by M. Lagro in [12] that the quantum Markov chain is convergent.

If we look at the proof of this theorem, we can generalize the technique to this general theorem in classical probability.

Theorem 3.1 *Let P_k be the Markov transition matrices on a finite states space Σ, suppose $\Pi P_k = P_k\Pi = \Pi$ for all k and $P_k \geq \delta_k\Pi$. If $\prod_{k=0}^{\infty}(1-\delta_k) = 0$, then $P_1 \cdots P_n \to \Pi$ as $n \to \infty$.*

Now, note that if our Q_k satisfies the conditions of Theorem 3.1, and therefore Proposition 3.3 holds, and this is more general than Proposition 3.3 extending the result to n by n matrices.

3.3 General case $m \times m$

The idea is to generalize the results to the general $m \times m$ case. Let's observe the following example.

Example 3.1 *Let* $G = \begin{bmatrix} 1 & 1 \\ 1 & 1 \end{bmatrix}$ *self-adjoint, and* U_n *a* 2×2 *unitary matrix such that* $U_n = e^{i\frac{G}{n\zeta}}$, *Note that* G *has the eigenvalues* $\lambda_1 = 2$ *and* $\lambda_2 = 0$ *with their eigenvectors* $v_1 = \begin{bmatrix} \frac{1}{\sqrt{2}} \\ \frac{1}{\sqrt{2}} \end{bmatrix}$ *and* $v_2 = \begin{bmatrix} \frac{1}{\sqrt{2}} \\ -\frac{1}{\sqrt{2}} \end{bmatrix}$.

So, with $A = \begin{bmatrix} \frac{1}{\sqrt{2}} & \frac{1}{\sqrt{2}} \\ \frac{1}{\sqrt{2}} & -\frac{1}{\sqrt{2}} \end{bmatrix}$. *We diagonalize*

$$G = A \begin{bmatrix} 2 & 0 \\ 0 & 0 \end{bmatrix} A^* = A \begin{bmatrix} 2 & 0 \\ 0 & 0 \end{bmatrix} A$$

Therefore, we have

$$e^{iG} = A \cdot \exp\left(i \begin{bmatrix} 2 & 0 \\ 0 & 0 \end{bmatrix}\right) \cdot A = \begin{bmatrix} e^{i2}r^2 + r^2 & e^{i2}r^2 - r^2 \\ e^{i2}r^2 - r^2 & e^{i2}r^2 + r^2 \end{bmatrix}$$

where $r = \frac{1}{\sqrt{2}}$, *which implies*

$$e^{i\frac{G}{\sqrt{n\zeta}}} = \begin{bmatrix} \frac{1}{2}\left(e^{i\frac{2}{\sqrt{n\zeta}}} + 1\right) & \frac{1}{2}\left(e^{i\frac{2}{\sqrt{n\zeta}}} - 1\right) \\ \frac{1}{2}\left(e^{i\frac{2}{\sqrt{n\zeta}}} - 1\right) & \frac{1}{2}\left(e^{i\frac{2}{\sqrt{n\zeta}}} + 1\right) \end{bmatrix}$$

$$\implies |U_n|^2 = |e^{i\frac{G}{\sqrt{n\zeta}}}|^2 = \begin{bmatrix} \frac{1}{4}|\left(e^{i\frac{2}{\sqrt{n\zeta}}} + 1\right)|^2 & \frac{1}{4}|\left(e^{i\frac{2}{\sqrt{n\zeta}}} - 1\right)|^2 \\ \frac{1}{4}|\left(e^{i\frac{2}{\sqrt{n\zeta}}} - 1\right)|^2 & \frac{1}{4}|\left(e^{i\frac{2}{\sqrt{n\zeta}}} + 1\right)|^2 \end{bmatrix}$$

Note that the off-diagonal terms are close to 0 *when* n *is large, and with* $\theta = \frac{2}{\sqrt{n^\zeta}}$

$$\frac{1}{4}|\big(e^{i\frac{2}{\sqrt{n^\zeta}}}-1\big)|^2 = \frac{1}{4}\big(e^{i\frac{2}{\sqrt{n^\zeta}}}-1\big)\big(e^{i\frac{2}{\sqrt{n^\zeta}}}-1\big) = \frac{1}{4}\big(2-e^{i\theta}-e^{-i\theta}\big) = \frac{1}{4}\big(2-2\cos\theta\big)$$

$$= \frac{1}{2}\big[1-\cos(\frac{2}{\sqrt{n^\zeta}})\big] \approx \frac{1}{2}\cdot\frac{1}{2}\big(\frac{2}{\sqrt{n^\zeta}}\big)^2 = \frac{1}{n^\zeta}$$

Therefore, with $\delta_n = \frac{2}{n^\zeta}$*, we have obtained*

$$|U_n|^2 \geq \delta_n \cdot \begin{bmatrix} \frac{1}{2} & \frac{1}{2} \\ \\ \frac{1}{2} & \frac{1}{2} \end{bmatrix}$$

and

$$\prod_{n=1}^{\infty}\alpha_n = \prod_{n=1}^{\infty}(1-\delta_n) \sim e^{-\sum_{n=1}^{\infty}\delta_n}$$

Now, we generalize the idea to high dimensional space. Let's consider $H = span\{|1\rangle, ..., |m\rangle\}$ with $m \in \mathbb{N}$, and $U_n = e^{i\frac{G}{\sqrt{n^\zeta}}}$ with G a $m \times m$ symmetric matrix such that there exists $\epsilon > 0$, $|G_{ij}| > \epsilon_0$ for all i, j with the following

$$\Phi_n(\rho) = \sum_{i=0}^{m} A_i U_n \rho U_n^* A_i^*$$

and

$$\rho_n = \Phi_n \cdots \Phi_1(\rho) \tag{3.6}$$

where $A_0 = \sqrt{1-p}I$ and $A_i = \sqrt{p}|i\rangle\langle i|$, $1 \leq i \leq m$, and let $\rho_0 = |i\rangle\langle i|$ fixed, and

$$P_n(j) = Tr\big(|j\rangle\langle j|\rho_n\big)$$

And assume that $T_1, T_2, ...$ are i.i.d. **Geo(p)**, and $\sigma_n = T_1 + \cdots T_n$, fix t, define $n_t = \max\{n : \sigma_n \leq t\}$.

So, we have

$$P_t(j) = Tr\big(|j\rangle\langle j|\rho_t\big) = E\Big[Q_1(i, j_1)Q_2(j_1, j_2)\cdots Q_{n_t}(j_{n_t-1}, j_{n_t})W(j_{n_t}, j)\Big]$$

where $Q_n(i,j) = E|\langle j|U_{\sigma_{n-1}+T_n}\cdots U_{\sigma_{n-1}+1}|i\rangle|^2$ and $W(i,j) = E\Big[|\langle j|U_t\cdots U_{\sigma_n+1}|i\rangle|^2\Big]$

The idea is to show

Proposition 3.4 *For all probability distribution V and $i, j = 1, 2, ..., m$, if $0 < \zeta \leq 1$ and $0 < p \leq 1$, then*

$$\sum_i V_i P_t(j) \to \pi_j = \frac{1}{m},$$

as $t \to \infty$.

Proof of 3.4: Observe that we can write

$$VQ_1\cdots Q_nW - \Pi = VQ_1\cdots Q_nW - VQ_1\cdots Q_n + VQ_1\cdots Q_n - \Pi$$

$$= VQ_1\cdots Q_n\big(W - I\big) + \big(VQ_1\cdots Q_n - \Pi\big)$$

Since $0 < \zeta \leq 1$, the second term tends to 0 as $n \to \infty$ by Theorem 3.1, and hence, it's enough to show that $W - I \to 0$ since $VQ_1\cdots Q_n$ is bounded.

$$W(i,j) = E|\langle j|U_t\cdots U_{\sigma_{n_t}+1}|i\rangle|^2 = E\big|\langle j|e^{\frac{iG}{\sqrt{t^\zeta}}}\cdots e^{\frac{iG}{\sqrt{(\sigma_{n_t}+1)^\zeta}}}|i\rangle\big|^2$$

$$= E\big|\langle j|e^{iG\sum_{k=\sigma_{n_t}+1}^{t}\frac{1}{\sqrt{k^\zeta}}}|i\rangle\big|^2$$

Note that if we show that $|\langle j|e^{iG\sum_{k=\sigma_{n_t+1}}^{t}\frac{1}{\sqrt{k\zeta}}}|i\rangle\big|^2 \to 0$ a.s. for $i \neq j$. By Dominated Convergence Theorem, $W(i,j) \to \delta_{ij}$, and we obtain the result.

Let's write $U_n = U_n^F + U_n^D$ for every n where U_n^F are the off-diagonal parts and U_n^D is the diagonal parts of U_n. So, for $i \neq j$,

$$|\langle j|e^{iG\sum_{k=\sigma_{n_t+1}}^{t}\frac{1}{\sqrt{k\zeta}}}|i\rangle\big|^2 = \Big|\sum_{l=\sigma_{N_t}+1}^{t}\langle j|U_t\cdots U_{l+1}U_l^F U_{l-1}^D\cdots U_{\sigma_{N_t}+1}^D|i\rangle\Big|^2$$

This expansion is made by $U\cdots U(U^F+U^D) = U\cdots UU^F + U\cdots U(U^F + U^D)U^D = \cdots$. By Cauchy-Schwarz,

$$\leq (t-\sigma_{N_t})\sum_{l=\sigma_{N_t}+1}^{t}\Big|\langle j|U_t\cdots U_{l+1}U_l^F U_{l-1}^D\cdots U_{\sigma_{N_t}+1}^D|i\rangle\Big|^2$$

By definition, we have $U_n = e^{\frac{iG}{\sqrt{n^\zeta}}}$, where G is symmetric m by m matrix and $|U_n| \leq 1$.

$$\leq (t-\sigma_{N_t})\sum_{l=\sigma_{N_t}+1}^{t}\Big|\langle j|U_t\cdots U_{l+1}U_l^F|i\rangle U_{l-1}(i,i)\cdots U_{\sigma_{N_t}+1}(i,i)\Big|^2$$

$$\leq (t-\sigma_{N_t})\sum_{l=\sigma_{N_t}+1}^{t}\Big|\sum_{k\neq i}\langle j|U_t\cdots U_{l+1}|k\rangle U_l(k,i)U_{l-1}(i,i)\cdots U_{\sigma_{N_t}+1}(i,i)\Big|^2$$

By Cauchy-Schwarz again,

$$\leq (t-\sigma_{N_t})\sum_{l=\sigma_{N_t}+1}^{t}(m-1)\sum_{k\neq i}\Big|\langle j|U_t\cdots U_{l+1}|k\rangle\Big|^2\Big|U_l(k,i)\Big|^2\Big|U_{l-1}(i,i)\cdots U_{\sigma_{N_t}+1}(i,i)\Big|^2$$

Using the fact that $\Big|\langle j|U_t\cdots U_{l+1}|k\rangle\Big|^2 \leq 1$, $\Big|U_l(k,i)\Big|^2 = \mathcal{O}(\frac{1}{l^\zeta})$, and

$$\Big|U_{l-1}(i,i)\cdots U_{\sigma_{N_t}+1}(i,i)\Big|^2 \leq 1,$$

we conclude

$$(t-\sigma_{N_t})\sum_{l=\sigma_{N_t}+1}^{t}(m-1)^2\mathcal{O}\big(\frac{1}{l^\zeta}\big)\leq(m-1)^2(t-\sigma_{N_t})^2\mathcal{O}\Big(\frac{1}{(\sigma_{N_t}+1)^\zeta}\Big)$$

Now, it's enough to prove that $\dfrac{(t-\sigma_{N_t})^2}{(\sigma_{N_t})^\zeta}\leq\dfrac{T_{N_t+1}^2}{(T_1+\cdots+T_{N_t})^\zeta}\to 0$ as. The first inequality is trivial, and note that

$$\sum_{n=1}^{\infty}P\Big(\Big|\frac{T_n^2}{n^\zeta}\Big|>\epsilon\Big)=\sum_{n=1}^{\infty}P\Big(T_n^2>n^\zeta\epsilon\Big)=\sum_{n=1}^{\infty}P\Big(\frac{T_1^{\frac{2}{\zeta}}}{\epsilon^{\frac{1}{\zeta}}}>n\Big)\leq E\big(\frac{T_1^{\frac{2}{\zeta}}}{\epsilon^{\frac{1}{\zeta}}}\big)+1<\infty$$

And by Borel-Cantelli Lemma

$$P\Big(\Big|\frac{T_n^2}{n^\zeta}\Big|>\epsilon\text{ i.o. }\Big)=0$$

Therefore

$$\frac{T_n^2}{n^\zeta}\to 0\text{ a.s.}$$

So, using the law of large numbers, we can conclude that

$$\frac{T_{n+1}^2}{(T_1+\cdots T_n)^\zeta}=\frac{\frac{T_{n+1}^2}{n^\zeta}}{(\frac{T_1+\cdots T_n}{n})^\zeta}\to\frac{0}{E(T_1)^\zeta}\text{ a.s.}$$

□

Therefore, we have the most general convergence theorem for decoherent quantum Markov chains as follows,

Theorem 3.2 *Suppose that* $|G_{ij}|\geq\epsilon_0$ *for all* i,j. *Let* $\rho_0=|i\rangle\langle i|$, *if* $0<\zeta\leq 1$ *and* $0<p\leq 1$, *then*

$$\rho_t\to\sum_{i=1}^{m}\Pi_i\cdot|i\rangle\langle i|$$

where $\Pi_i=\frac{1}{m}$, *for* $i=1,...,m$.

Proof of 3.2: First, consider $\mu_t(j) = Tr\big(|j\rangle\langle j|\rho_t\big)$, and we show that $\mu_t \to \Pi$.

Note that

$$\mu_t(j) = \sum_{i_1,\dots i_t=0}^{m} Tr\Big(\langle j|A_{i_t}U_{i_t}\cdots A_{i_1}U_{i_1}|i\rangle\langle i|A_{i_1}^*U_{i_1}^*\cdots A_{i_t}^*U_{i_t}^*|j\rangle\Big)$$

$$= \sum_{i_1,\dots i_t=0}^{m} \Big|\langle j|A_{i_t}U_{i_t}\cdots A_{i_1}U_{i_1}|i\rangle\Big|^2$$

$$= \sum_{n=0}^{\infty} \sum_{0<\sigma_1<\cdots<\sigma_n\le t} \sum_{j_1,\dots j_n=1}^{m} \Big|\langle j|U_t\cdots U_{\sigma_n+1}|j_n\rangle\langle j_n|U_{\sigma_n}\cdots U_{\sigma_{n-1}+1}|j_{n-1}\rangle\cdots$$

$$\cdots\langle j_1|U_{\sigma_1}\cdot\cdots\cdot U_1|i\rangle\Big|^2 q^{t-n}p^n$$

$$= \sum_{n=0}^{\infty} \sum_{0<\sigma_1<\cdots<\sigma_n\le t} \sum_{j_1,\dots j_n=1}^{m} \Big|\langle j|U_t\cdots U_{\sigma_n+1}|j_n\rangle\Big|^2 q^{t-\sigma_n-1}p\times$$

$$\times\Big|\langle j_n|U_{\sigma_n}\cdots U_{\sigma_{n-1}+1}|j_{n-1}\rangle\Big|^2 q^{\sigma_n-\sigma_{n-1}-1}p\cdots\Big|\langle j_1|U_{\sigma_1}\cdots U_1|i\rangle\Big|^2 q^{\sigma_1-1}p$$

Consider $T_1, T_2, \dots$ iid geometric(p), $\sigma_n = T_1 + \cdots T_n$,

$$N_t = \max\{n \ge 0, \sigma_n \le t\}$$

$$Q_n(i,j) = E\Big[\big|\langle j|U_{\sigma_n}\cdots U_{\sigma_{n-1}+1}|i\rangle\big|^2\Big]$$

$$W(i,j) = E\Big[\big|\langle j|U_{\sigma_t}\cdots U_{\sigma_{N_t}+1}|i\rangle\big|^2\Big]$$

So, we also consider

$$\mu_t(j) = E\Big[\sum_{j_1,\dots,j_{N_t}=1}^{m} \big|\langle j|U_t\cdots U_{\sigma_{N_t}+1}|j_{N_t}\rangle\big|^2\big|\langle j_{N_t}|U_{\sigma_{N_t}}\cdots U_{\sigma_{N_t-1}+1}|j_{N_t-1}\rangle\big|^2\cdots$$

$$\cdots\big|\langle j_1|U_{\sigma_1}\cdots U_1|i\rangle\big|^2\Big],$$

and $\nu_t(j) = E\Big[\sum_{j_1,\dots,j_{N_t}=1}^{m} \big|\langle j_{N_t}|U_{\sigma_{N_t}}\cdots U_{\sigma_{N_t-1}+1}|j_{N_t-1}\rangle\big|^2\cdots\big|\langle j_1|U_{\sigma_1}\cdots U_1|i\rangle\big|^2\Big]$

Let $Q_{k,l}(i,j) = \big|\langle j|U_l \cdots U_{k+1}|i\rangle\big|^2$, we write

$$\nu_t(j) = E\Big[\big(Q_{1,\sigma_1}Q_{\sigma_1,\sigma_2}\cdots Q_{\sigma_{N_t-1},\sigma_{N_t}}\big)(i,j)\Big]$$

Note that the Cauchy Criterium $\|Q_{\sigma_m,\sigma_{m+1}}\cdots Q_{\sigma_{n-1},\sigma_n} - I\| \to 0$ a.s. implies

$$\lim_{n\to\infty} Q_{1,\sigma_1}Q_{\sigma_1,\sigma_2}\cdots Q_{\sigma_{n-1},\sigma_n} = \prod_{s=1}^{\infty} Q_{\sigma_{s-1},\sigma_s},\ a.s$$

where $\sigma_0 = 1$, now, since $N_t \to \infty$ when $t \to \infty$, we obtain

$$\lim_{t\to\infty} Q_{1,\sigma_1}Q_{\sigma_1,\sigma_2}\cdots Q_{\sigma_{N_t-1},\sigma_{N_t}} = \prod_{s=1}^{\infty} Q_{\sigma_{s-1},\sigma_s} \quad \text{a.s.}$$

Therefore, by BCT and independence, when $t \to \infty$

$$\nu_t(j) \to E\Big[\prod_{s=1}^{\infty} Q_{\sigma_{s-1},\sigma_s}\Big] = \prod_{s=1}^{\infty} E\Big[Q_{\sigma_{s-1},\sigma_s}\Big](i,j) = \lim_{n\to\infty}\prod_{s=1}^{n} E\Big[Q_{\sigma_{s-1},\sigma_s}\Big](i,j)$$

Since we have defined $Q_n(i,j) = E\Big[\big|\langle j|U_{\sigma_n}\cdots U_{\sigma_{n-1}+1}|i\rangle\big|^2\Big]$,

$$\lim_{n\to\infty}\prod_{s=1}^{n} E\Big[Q_{\sigma_{s-1},\sigma_s}\Big](i,j) = \lim_{n\to\infty} Q_1Q_2\cdots Q_n(i,j) = \Pi(i,j)$$

Now,

$$\big|\mu_t(j) - \nu_t(j)\big| \leq$$

$$\leq \Big|E\big[\big(Q_{1,\sigma_1}Q_{\sigma_1,\sigma_2}\cdots Q_{\sigma_{N_t-1},\sigma_{N_t}}\big)(i,j)\big] - E\big[\big(Q_{1,\sigma_1}Q_{\sigma_1,\sigma_2}\cdots Q_{\sigma_{N_t-1},\sigma_{N_t}}\big)(i,j)\big]\Big|$$

$$\leq \Big|E\big[\big(Q_{1,\sigma_1}Q_{\sigma_1,\sigma_2}\cdots Q_{\sigma_{N_t-1},\sigma_{N_t}}Q_{\sigma_{N_t},t}\big)(i,j) - \big(Q_{1,\sigma_1}Q_{\sigma_1,\sigma_2}\cdots Q_{\sigma_{N_t-1},\sigma_{N_t}}\big)(i,j)\big]\Big|$$

$$\leq E\Big|Q_{1,\sigma_1}Q_{\sigma_1,\sigma_2}\cdots Q_{\sigma_{N_t-1},\sigma_{N_t}}\big(Q_{\sigma_{N_t},t} - I\big)(i,j)\Big|$$

Note that as $t \to \infty$

$$\big\|Q_{1,\sigma_1}Q_{\sigma_1,\sigma_2}\cdots Q_{\sigma_{N_t-1},\sigma_{N_t}}\big(Q_{\sigma_{N_t},t} - I\big)\big\|_{\infty}$$

$$\leq \|Q_{1,\sigma_1}\|_\infty \|Q_{\sigma_1,\sigma_2}\|_\infty \cdots \big\|Q_{\sigma_{N_t-1},\sigma_{N_t}}\big\|_\infty \big\|Q_{\sigma_{N_t},t} - I\big\|_\infty \leq \big\|Q_{\sigma_{N_t},t} - I\big\|_\infty \to 0$$

By Bounded Convergence Theorem, $\big(Q_{\sigma_{N_t},t} - I\big)(i,j) \to 0$ a.s., and therefore $\big|\mu_t(j) - \nu_t(j)\big| \to 0$.

We have proved that if $\rho_0 = |i\rangle\langle i|$, then $Tr\big(|j\rangle\langle j|\rho_t\big) \to \Pi_j$, let's show now

$$\rho_t \to \sum_{j=1}^{m} \pi_j \cdot |j\rangle\langle j|.$$

Enough to show that $Tr\big(|k\rangle\langle j|\rho_t\big) \to 0$ for all $k \neq j$. We can see that

$$Tr\big(|k\rangle\langle j|\rho_t\big) = \langle j|\rho_t|k\rangle = \langle j|\Phi_t \cdots \Phi_2\Phi_1|i\rangle\langle i|k\rangle$$

$$= \sum_{i_1,i_2,\ldots,i_t=0}^{m} \langle j|A_{i_t}U_t \cdots A_{i_1}U_1|i\rangle\langle i|U_1^*A_{i_1}^* \cdots U_t^*A_{i_t}^*|k\rangle$$

$$= E\Big[\sum_{j_1,\ldots,j_{N_t}=1}^{m} \langle j|U_t \cdots U_{\sigma N_t+1}|j_{N_t}\rangle\langle j_{N_t}|U_{\sigma N_t} \cdots U_{\sigma N_t-1+1}|j_{N_t-1}\rangle \cdots$$

$$\cdots \langle j_1|U_{\sigma_1} \cdots U_2U_1|i\rangle\langle i|U_1^*U_2^* \cdots U_{\sigma_1}^*|i\rangle \cdots \langle j_{N_t-1}|U_{\sigma_{N_t-1}}^* \cdots U_{\sigma_{N_t}}^*|j_{N_t}\rangle \times$$

$$\times \langle j_{N_t}|U_{\sigma_{N_t}+1}^* \cdots U_t^*|k\rangle\Big]$$

$$= E\Big[\sum_{j_1,\ldots,j_{N_t}=1}^{m} \langle j|U_t \cdots U_{\sigma N_t+1}|j_{N_t}\rangle(Q_{1\sigma_1}Q_{\sigma_1\sigma_2} \cdots Q_{\sigma_{N_t-1}\sigma_{N_t}})(i,j_{N_t}) \times$$

$$\times \langle j_{N_t}|U_{\sigma_{N_t}+1}^* \cdots U_t^*|k\rangle\Big]$$

Now, we define

$$W(i,j,k) := \langle j|U_t \cdots U_{\sigma_{N_t}+1}|i\rangle\langle i|U_{\sigma_{N_t}+1}^* \cdots U_t^*|k\rangle$$

$$= \langle j|U_t \cdots U_{\sigma_{N_t}+1}|i\rangle\overline{\langle k|U_t \cdots U_{\sigma_{N_t}+1}|i\rangle}$$

So, we have that

$$Tr\big(|k\rangle\langle j|\rho_t\big) = E\big[Q_{1\sigma_1}Q_{\sigma_1\sigma_2}\cdots Q_{\sigma_{N_t-1}\sigma_{N_t}}W\big](i,j,k)$$

We define

$$|QW(i,j,l)| := \big|\sum_l Q(i,l)W(l,j,k)\big|$$

$$\leq \sup_l ||w(l,j,l)|\sum_l Q(i,l) = \sup_l |w(l,j,k)| \to 0$$

as $t \to$ for all $j \neq k$. Since either j or $k \neq l$, and $\zeta > 0$, suppose that $j \neq l$

$$\big|\langle j|U_t\cdots U_{\sigma_{N_t+1}}|l\rangle\big|^2 \to 0$$

and

$$\big|\langle k|U_t\cdots U_{\sigma_{N_t}}|l\rangle\big|^2 \leq 1$$

□

3.4 Numerical simulations

Let's go back to the path integral formula defined in Definition 3.2 and the Equation (3.5), and this leads us to the following algorithms for 2 dimensional case, $H = span\{|1\rangle, |2\rangle\}$, to generate the numerical simulations:

Step 1: Generate $T_1, T_2, ..., T_n$ iid with geometric distribution with a given $0 < p \leq 1$.

Step 2: Define $\sigma_0 = 0, \sigma_1 = T_1, ..., \sigma_n = T_1 + \cdots + T_n$

Step 3: For each k, calculate $Q_{\sigma_k,\sigma_{k+1}}(i,j) = |\langle j|U_{\sigma_{k+1}} \cdots U_{\sigma_k+1}|i\rangle|^2$

Step 4: Fix t, and $\sigma_{N_t} \leq t < \sigma_{N_t+1}$, define $W_{\sigma_{N_t},t}(i,j) = |\langle j|U_t \cdots U_{\sigma_{N_t}+1}|i\rangle|^2$

Step 5: Compute the matrix $Q_{0,\sigma_1}Q_{\sigma_1,\sigma_2} \cdots Q_{\sigma_{N_t-1},\sigma_{N_t}}W_{\sigma_{N_t},t}$

Step 6: Run the k samples of the simulation and calculate the mean.

Step 7: Calculate the absolute value of the difference between the mean from step 6. and the matrix $\begin{pmatrix} \frac{1}{2} & \frac{1}{2} \\ \frac{1}{2} & \frac{1}{2} \end{pmatrix}$ for each time t.

Some Python codes for basic operator calculations will be annexed in Appendix B. We assume that $\lambda = \frac{1}{2}$, and run 1000 samples for 5000 time steps.

First, we consider the case $\zeta = 0.8$, we can observe that the simulation results with different values of p shown in Figures 3.1, 3.2, and 3.3 that the absolute value of the difference between the matrix product obtained and the equilibrium matrix $\begin{pmatrix} \frac{1}{2} & \frac{1}{2} \\ \frac{1}{2} & \frac{1}{2} \end{pmatrix}$ converges to 0 which is in accord with the convergence theorems we proved. Moreover, quantum mechanics intuition tells us that if p is closer to 0, less decoherent, the convergence phenomenon to the classical result should not be clear. This can be observed in Figure 3.3, that the convergence is slower compared with Figures 3.1 and 3.2. In other words, if the probability of the quantum system to be measured is closer to 0, the system will converge slowly.

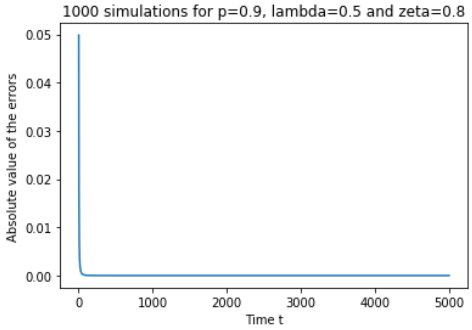

Figure 3.1: Quantum Markov chain convergence for $\zeta = 0.8$ and $p = 0.9$

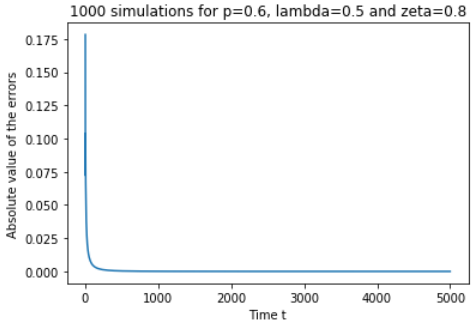

Figure 3.2: Quantum Markov chain convergence for $\zeta = 0.8$ and $p = 0.6$

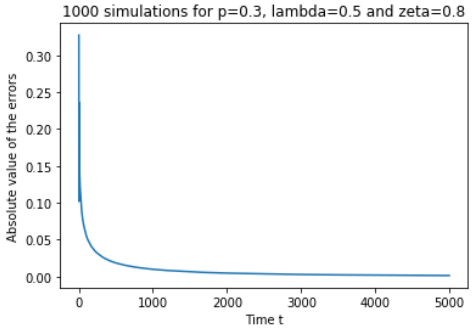

Figure 3.3: Quantum Markov chain convergence for $\zeta = 0.8$ and $p = 0.3$

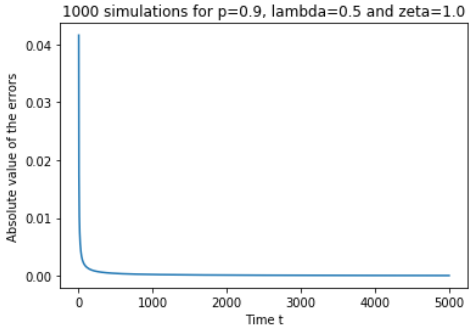

Figure 3.4: Quantum Markov chain convergence for $\zeta = 1$ and $p = 0.9$

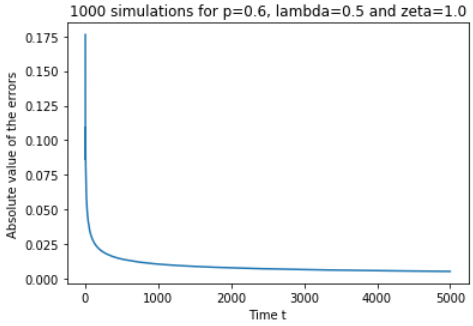

Figure 3.5: Quantum Markov chain convergence for $\zeta = 1$ and $p = 0.6$

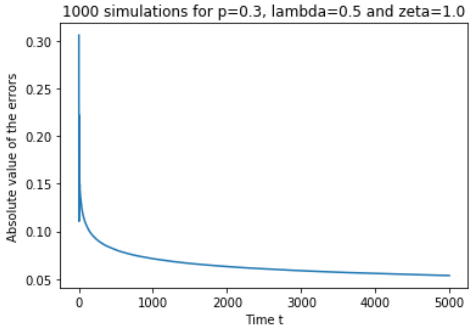

Figure 3.6: Quantum Markov chain convergence for $\zeta = 1$ and $p = 0.3$

Another interesting example to analyze is when $\zeta = 1$. We can observe from Figures 3.4, 3.5, and 3.6 that the convergence is slower than the case $\zeta = 0.8$.

CHAPTER 4

TIME-INHOMOGENEOUS QUANTUM RANDOM WALKS

Percolation as a mathematical theory was introduced by Broadbent and Hammersley [2], and it is applied to model probabilities which are affected by different environment. For instance space-inhomogeneous random walk on $\mathbb{Z}$, the probability of each step depends on the state position in $\mathbb{Z}$. However, instead of the space, the probability can only depends on the time step. Let's define the inhomogeneuous quantum analogue of the random walk on the infinite discrete space $\mathbb{Z}$. Avoiding the confusion with the notations in Chapter 3, we will use $\hat{}$ for the operators in this chapter. We let $H = H_p \otimes H_c$ and for

$n = 1, 2, ...$, $\hat{F}_n : H \to H$ be a inhomogeneous unitary transformation on H defined by

$$\hat{F}_n = \sum_{x \in Z} |x\rangle\langle x| \otimes C_{n,x}, \tag{4.1}$$

where $C_{n,x} : H_c \to H_c$ are unitary operators which depend on the time n and the position x.

Generalizing from Definition 2.4, the inhomogeneous evolution operator at time n of quantum random walk is given by

$$\hat{U}_n = S\hat{F}_n, \tag{4.2}$$

where $S = S_o$ for a standard quantum random walk, and $S = S_f$ for the flip-flop quantum random walk.

Similarly to homogeneous quantum walk defined in Chapter 2. Let $|\psi_0\rangle \in H$. Then $|\psi_t\rangle = \hat{U}_t ... \hat{U}_2 \hat{U}_1 |\psi_0\rangle$ is called an inhomogeneous quantum random walk with initial state $|\psi_0\rangle$. The probability that at time t, the quantum random walk is observed at state $|x^i\rangle$ is defined by

$$\hat{p}_t(x^i) = |\langle x^i|\psi_t\rangle|^2, \tag{4.3}$$

and the probability that at time t, the quantum random walk is observed at state $|x\rangle$ is defined by

$$\hat{p}_t(x) = \sum_i |\langle x^i|\psi_t\rangle|^2. \tag{4.4}$$

For decoherent time-inhomogeneous quantum random walks, we suppose the quantum walk starts at the state $|0\rangle \otimes |\Phi_0\rangle$, then, the initial state is given by the density operator

$$\hat{\rho}_0 = |0\rangle\langle 0| \otimes |\Phi_0\rangle\langle\Phi_0| = (|0\rangle \otimes |\Phi_0\rangle)(\langle 0| \otimes \langle\Phi_0|). \tag{4.5}$$

After t steps, with the decoherence measurement $\{A_n\}_{n\in\mathbb{N}}$, the state evolves to

$$\hat{\rho}_t = \sum_{n_1,\ldots,n_t} A_{n_t}\hat{U}_t \cdots A_{n_1}\hat{U}_1(|0\rangle \otimes |\Phi_0\rangle)(\langle 0| \otimes \langle\Phi_0|)\hat{U}_1^* A_{n_1}^* \cdots \hat{U}_t^* A_{n_t}^* \tag{4.6}$$

$$= \sum_n A_n \hat{U}_t \hat{\rho}_{t-1} \hat{U}_t^* A_n^* \tag{4.7}$$

The probability that at time t, the decoherent inhomogeneous quantum random walk is observed at state $|x^i\rangle$ is defined by

$$\hat{p}_t(x^i) = Tr([|x^i\rangle\langle x^i|]\hat{\rho}_t) \tag{4.8}$$

and the probability that at time t, the quantum random walk is observed at state $|x\rangle$ is defined by

$$\hat{p}_t(x) = \sum_i p_t(x^i) = Tr([|x\rangle\langle x| \otimes I_c]\hat{\rho}_t) \tag{4.9}$$

If the unitary operator depends on the position or the time, the quantum walk is called inhomogeneous quantum walk, here we have some examples of position-inhomogenuous quantum walk and time-inhomogenuous quantum walks,

Example 4.1 *Let $S = S_f$, and $C_{n,x} = C_x$ depends on the position such that*

$$C_x = \begin{bmatrix} (\frac{1}{1+|x|})^{1/2} & (1-\frac{1}{1+|x|})^{1/2} \\ (1-\frac{1}{1+|x|})^{1/2} & -(\frac{1}{1+|x|})^{1/2} \end{bmatrix}$$

Then the quantum random walk is called the flip-flop quantum random walk with linear drift.

Example 4.2 *Let $S = S_o$, and $C_{n,x} = C_x$ depends on the position such that*

$$C_x = \begin{bmatrix} (\frac{1}{1+|x|})^{1/2} & (1-\frac{1}{1+|x|})^{1/2} \\ (1-\frac{1}{1+|x|})^{1/2} & -(\frac{1}{1+|x|})^{1/2} \end{bmatrix}$$

Then the quantum random walk is called the standard quantum random walk with linear drift.

Example 4.3 *Let $S = S_o$, and $C_{n,x} = C_n$ depends on the time step such that*

$$C_n = \begin{bmatrix} \sqrt{1-\frac{\lambda}{n^\zeta}} & \sqrt{\frac{\lambda}{n^\zeta}} \\ \sqrt{\frac{\lambda}{n^\zeta}} & -\sqrt{1-\frac{\lambda}{n^\zeta}} \end{bmatrix}$$

where λ and ζ are non negative real numbers.

4.1 Time-inhomogenuous quantum walk and its path integral expression

We now concentrate on analyzing the decoherent time-inhomogeneous quantum walk defined with unitary operators in Example 4.3, and the total decoherence measurement defined in Example 2.4. We have with the initial density

operator $\rho_0 = |0\rangle\langle 0| \otimes |\Phi_0\rangle\langle\Phi_0|$, and the decoherence measurement

$$\{A_{xi}; x \in Z^1, i = 1, 2\} \cup \{A_0\}$$

where for $p \in [0, 1]$, $x \in \mathbb{Z}$, and $i = 1, 2$

$$A_{xi} = \sqrt{p} \cdot |x\rangle\langle x| \otimes |i\rangle\langle i|,$$

and

$$A_0 = \sqrt{1-p} \cdot I_p \otimes I_c.$$

Then our time inhomogeneous quantum walk with total decoherence measurement with decoherence parameter p is defined as

$$\hat{\rho}_t = A_0 \hat{U}_t \hat{\rho}_{t-1} \hat{U}_t^* A_0^* + \sum_{x,i} A_{x,i} \hat{U}_t \hat{\rho}_{t-1} \hat{U}_t^* A_{x,i}^* \tag{4.10}$$

with the time-inhomogeneous unitary operators

$$C_n = \begin{bmatrix} \sqrt{1 - \frac{\lambda}{n^\zeta}} & \sqrt{\frac{\lambda}{n^\zeta}} \\ \sqrt{\frac{\lambda}{n^\zeta}} & -\sqrt{1 - \frac{\lambda}{n^\zeta}} \end{bmatrix} \tag{4.11}$$

where $\lambda, \zeta > 0$.

Let T_1, T_2... geometric random variables with probability p with $\sigma_1 = T_1$,..., $\sigma_n = T_1 + ... + T_n$, and $\rho_0 = |0\rangle\langle 0| \otimes |i_0\rangle\langle i_0|$, we have that the probability after t steps at the position x

$$\hat{p}_t(x) = \sum_{j=1}^{2} Tr\Big(|x\rangle\langle x| \otimes |j\rangle\langle j| \hat{\rho}_t\Big)$$

Let's recall the Q_n's defined in Definition 3.1 using the time-inhomogeneous operators above in (4.11)

$$Q_n(i,j) := E\Big[\big|\langle j|C_{\sigma_{n-1}+T_n}\cdots C_{\sigma_{n-1}+1}|i\rangle\big|^2\Big], \tag{4.12}$$

and, for discrete infinite space quantum walks, we generalize the idea to the following definition,

Definition 4.1 *Let $\hat{Q}_{\sigma_i\sigma_{i+1}}(x,y,i,j)$ the probability from x to the state y on the position space, and i to j on the coin space during the time σ_i to σ_{i+1}, and $\hat{W}(x,y,i,j)$ the probability from x to the state y on the position space, and i to j on the coin space during the time σ_n to t, which is*

$$\hat{Q}_{\sigma_k,\sigma_{k+1}}(x,y,i,j) = |\langle y,j|\hat{U}_{\sigma_{k+1}}\cdots\hat{U}_{\sigma_k+1}|x,i\rangle|^2$$

$$\hat{W}_{\sigma_{N_t},t}(x,y,i,j) = |\langle y,j|\hat{U}_t\cdots\hat{U}_{\sigma_{N_t}}|x,i\rangle|^2$$

where $x,y\in\mathbb{Z}$, and $i,j=1,2$

Therefore, we have the probability at x after t time steps using the path integral expression, by coin-space decoherence

$$\hat{p}_t(x) = \sum_{j=1}^{2} E\Big[\sum_{x_1,\ldots,x_{\sigma_{N_t}}\in\mathbb{Z}}\sum_{i_1,\ldots i_{N_t}\in\{1,2\}}\hat{Q}_{\sigma_0\sigma_1}(0,i_0,x_1,i_1)\cdots$$

$$\cdots\hat{Q}_{\sigma_{N_t-1}\sigma_{N_t}}(x_{\sigma_{N_t}-1},i_{\sigma_{N_t}-1},x_{N_t},i_{N_t})\hat{W}_{\sigma_{N_t},t}(x_{\sigma_{N_t}},i_{\sigma_{N_t}},x,j)\Big]$$

Note that using the translation invariant property

$$\hat{Q}_{\sigma_i\sigma_{i+1}}(x,i,y,j) = \hat{Q}_{\sigma_i\sigma_{i+1}}(0,i,y-x,j),$$

$$\hat{W}_{\sigma_{N_t},t}(x,i,y,j) = \hat{W}_{\sigma_{N_t},t}(0,i,y-x,j)$$

Let's just denote

$$\hat{Q}_{\sigma_i\sigma_{i+1}}(x,i,j) := \hat{Q}_{\sigma_i\sigma_{i+1}}(0,i,x,j),$$

and

$$\hat{W}_{\sigma_{N_t},t}(x,i,j) := \hat{W}_{\sigma_{N_t},t}(0,i,x,j),$$

and define for $i,j \in \{1,2\}$

$$R_{\sigma_k\sigma_{k+1}}(i,j) := \sum_{x\in\mathbb{Z}} \hat{Q}_{\sigma_k\sigma_{k+1}}(x,i,j)$$

$$\tilde{R}_{\sigma_{N_t},t}(i,j) := \sum_{x\in\mathbb{Z}} \hat{W}_{\sigma_{N_t},t}(x,i,j)$$

And, we obtain the path integral expression for $\hat{p}_t(x)$,

$$\hat{p}_t(x) = \sum_{j=1}^{2} E\Big[\sum_{x_1,\ldots,x_k} \sum_{i_1,\ldots i_k} \frac{\hat{Q}_{\sigma_0\sigma_1}(x_1,i_0,i_1)}{R_{\sigma_0\sigma_1}(i,i_1)} \cdots \frac{\hat{Q}_{\sigma_{N_t-1}\sigma_{N_t}}(x_k-x_{k-1},i_{k-1},i_k)}{R_{\sigma_{N_t-1}\sigma_{N_t}}(i_{k-1},i_k)} \cdot$$

$$\cdot \frac{\hat{W}_{\sigma_{N_t}t}(x-x_k,i_k,j)}{\tilde{R}_{\sigma_{N_t}t}(i_k,j)} \cdot R_{\sigma_0\sigma_1}(i_0,i_1)\cdots R_{\sigma_{N_t-1},\sigma_{N_t}}(i_{\sigma_{N_t}-1},i_{\sigma_{N_t}})\tilde{R}_{\sigma_{N_t}t}(i_k,j)\Big]$$

4.2 Representation theorem

Now, suppose that I_k is the Markov chain defined by $I_0 = i_0$ with the property that $P(I_{k+1} = j | I_k = i) = R_{\sigma_k\sigma_{k+1}}(i,j)$, and $\tilde{I}_t$ such that $P(I_t = j | I_{N_t} = i) = \tilde{R}_{\sigma_{N_t}t}(i,j)$. Also let $\mu_{\sigma_k\sigma_{k+1}}(\cdot,i,j)$ and $\tilde{\mu}_{\sigma_{N_t}t}(\cdot,i,j)$ be probability distributions on $\mathbb{Z}$ for $i,j = 1,2$ defined as

$$\mu_{\sigma_k\sigma_{k+1}}(x,i,j) := \frac{\hat{Q}_{\sigma_k,\sigma_{k+1}}(x,i,j)}{\sum_{x\in\mathbb{Z}} \hat{Q}_{\sigma_k,\sigma_{k+1}}(x,i,j)},$$

and

$$\tilde{\mu}_{\sigma_{N_t}t}(x,i,j)=\frac{\hat{W}_{\sigma_{N_t},t}(x,i,j)}{\sum_{x\in\mathbb{Z}}\hat{W}_{\sigma_{N_t},t}(x,i,j)},$$

Let $Y_{\sigma_k,\sigma_{k+1}}(i,j)$ independent random variables with distributions $\mu_{\sigma_k\sigma_{k+1}}(\cdot,i,j)$, and $\tilde{Y}_{\sigma_{N_t},t}(i,j)$ random variable with distribution $\tilde{\mu}_{\sigma_{N_t}t}(\cdot,i,j)$. We have

$$\begin{aligned}\hat{p}_t(x)&=\sum_{j=1}^{2}E^{\sigma}E^{Y}\Big(\mathbb{1}_x\big[Y_{\sigma_0\sigma_1}(i_0,i_1)+Y_{\sigma_1\sigma_2}(i_1,i_2)+\cdots+Y_{\sigma_{N_t-1}\sigma_{N_t}}(i_{k-1},i_k)+\\&\quad+\tilde{Y}_{\sigma_{N_t}t}(i_k,j)\big]\cdot\big[R_{\sigma_0\sigma_1}(i_0,i_1)\cdots R_{\sigma_{N_t-1}\sigma_{N_t}}(i_{k-1},i_k)\cdot\tilde{R}_{\sigma_N t}(i_k,j)\big]\Big)\\&=E^{\sigma}E^{I}E^{Y}\Big(\mathbb{1}_x\Big[Y_{\sigma_0\sigma_1}(i_0,I_1)+Y_{\sigma_1\sigma_2}(I_1,I_2)+\cdots+Y_{\sigma_{N_t-1}\sigma_{N_t}}(I_{N_t-1},I_{N_t})+\\&\quad+\tilde{Y}_{\sigma_{N_t}t}(I_{N_t},I_t)\Big]\Big)\end{aligned}$$

We have proved the following representation theorem,

Theorem 4.1 (σ-I-Y representation theorem) *Let the initial state be $|0\rangle\otimes|i_0\rangle$, then the probability of the time-inhomogeneous quantum walk defined in (4.10) and (4.11) is found in x is*

$$\hat{p}_t(x)=E^{\sigma}E^{I}E^{Y}\Big(\mathbb{1}_x\Big[Y_{\sigma_0\sigma_1}(i_0,I_1)+Y_{\sigma_1\sigma_2}(I_1,I_2)+\cdots+Y_{\sigma_{N_t-1}\sigma_{N_t}}(I_{N_t-1},I_{N_t})+\\+\tilde{Y}_{\sigma_{N_t}t}(I_{N_t},I_t)\Big]\Big)$$

Remark 4.1 *Theorem 4.1 not only gives us a new formula about calculating the probability of a quantum random walk to be found in x at time t, but also a better visualization of it using path integral expression connecting quantum*

probability and classical analytic probability. We will discuss some applications and examples for the theorem in Section 4.3.

4.3 Applications and examples

Theorem 4.1 can directly imply the following Monte Carlo simulation algorithms to estimate the probability at x and the distribution of the decoherent quantum walk at time t.

4.3.1 Algorithms

Following the proof of Theorem 4.1, and using the same notations, we have

Step 1: Fix t, generate $T_1, T_2, ..., T_n, T_{n+1}$ iid with geometric distribution with probability p, and let $\sigma_0 = 0, \sigma_1 = T_1, ..., \sigma_{n+1} = T_1 + \cdots + T_{n+1}$, and suppose that $\sigma_n < t < \sigma_{n+1}$.

Step 2: Let $\hat{Q}_{\sigma_k,\sigma_{k+1}}(x,i,j) = |\langle x,j|\hat{U}_{\sigma_{k+1}} \cdots \hat{U}_{\sigma_k+1}|0,i\rangle|^2$, and $\hat{W}_{\sigma_n,t}(x,i,j) = |\langle x,j|\hat{U}_t \cdots \hat{U}_{\sigma_n}|0,i\rangle|^2$ where $x \in \mathbb{Z}$, and $i,j = 1,2$.

Step 3: Using the $\hat{Q}_{\sigma_k,\sigma_{k+1}}$ and $\hat{W}_{\sigma_n,t}$ from the previous step to generate Y_{k+1}, independent random variables with distribution $\mu_{\sigma_k\sigma_{k+1}}(\cdot,i,j)$, and $\tilde{Y}_t$ random variable with distribution $\tilde{\mu}_{\sigma_n,t}(.,i,j)$.

Step 4: Fix i, and j, generate $Z_t(i,j) = Y_1(i,j) + Y_2(i,j) + \cdots + Y_n(i,j) + \tilde{Y}_t(i,j)$

Step 5: Generate different samples of the Markov chain $I_0 = i_0$, $\{I_k\}_{k=0}^n$, and I_t with the transition $P(I_{k+1} = j|I_k = i) = R_{\sigma_k\sigma_{k+1}}(i,j)$, and $P(I_t = j|I_n = i) = \tilde{R}_{\sigma_n,t}(i,j)$ for each Markov chain I_t generate sample for $Z_t(i_0, I_t)$.

Step 6: Repeat the procedure with different samples of $\{\sigma_n\}$, and take the average over Y, I, and σ, then we obtain the probability for each $x \in \mathbb{Z}$, and the distribution of the decoherent quantum walk at time t.

We run the simulation using the algorithm with different values of λ, ζ, and p in Python, and following examples show that the simulated scaling limits accord with the theoretical results proven. Some basic operators codes will be annexed in Appendix B.

4.3.2 Approximation of classical probability distribution densities

We note that if $p = 1$, the probability to make the measurement at each step is 1 which means that the decoherent quantum walk becomes a classical probability random walk with time-inhomogeneous transition matrix

$$C_n = \begin{bmatrix} 1 - \frac{\lambda}{n^\zeta} & \frac{\lambda}{n^\zeta} \\ \frac{\lambda}{n^\zeta} & 1 - \frac{\lambda}{n^\zeta} \end{bmatrix},$$

and J. Englander and S. Volkov in [6] proved that if $\zeta = 1$, the scaling limit

$$\hat{p}(x,t) \equiv p_d(tx,t),\ x \in \frac{\mathbb{Z}}{t}$$

converges to the symmetric Beta distribution, **Beta(λ,λ)**, in $[-1, 1]$. In particular, $\hat{p}(x, t)$ converges to arcsine law, uniform law and semicircle law when $\lambda = \frac{1}{2}, 1, \frac{3}{2}$ respectively.

Therefore in our model, with $p = 1$ and respective parameters above, our algorithms can generates the approximations of these distributions. By taking large samplings numbers and time scales, the generated approximated distributions will converge to the theoretical distributions. With $t = 500$, Figure 4.1, Figure 4.2 and Figure 4.3 show the obtained approximated arcsine, uniform, and semicircle laws in the interval $[-1, 1]$

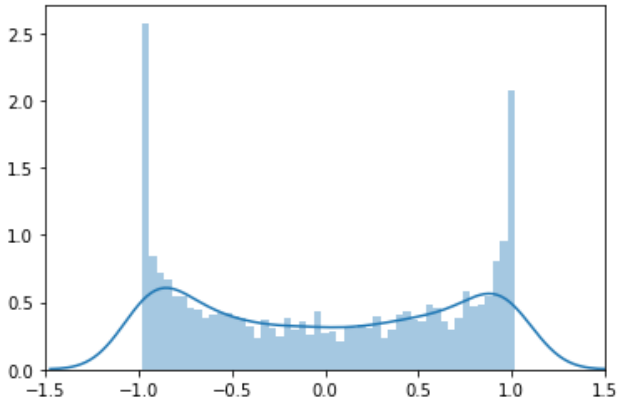

Figure 4.1: Approximated arcsine law for $\zeta = 1$, $\lambda = \frac{1}{2}$ and $p = 1$

Another interesting case is when $\sum \frac{\lambda}{n^\zeta} < \infty$, theory shows that

$$\hat{p}(x, t) \equiv p_d(tx, t), \ x \in \frac{\mathbb{Z}}{t}$$

converges to **Bernoulli($\frac{1}{2}$)** by Borel-Cantelli Lemma [6] as we can see in Figure 4.4.

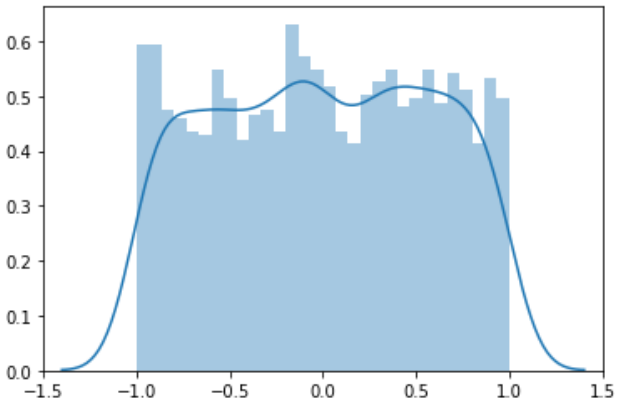

Figure 4.2: Approximated uniform law for $\zeta = 1$, $\lambda = 1$ and $p = 1$

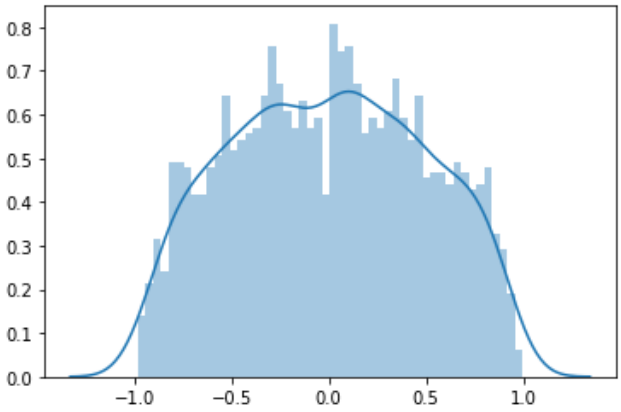

Figure 4.3: Approximated semicircle law for $\zeta = 1$, $\lambda = \frac{3}{2}$ and $p = 1$

4.3.3 Approximation of decoherent Hadamard walk

We can observe that if $\zeta = 0$, the model becomes a decoherent homogeneous quantum walk. For instance, by taking $\zeta = 0$ and $\lambda = \frac{1}{2}$, the unitary operators will be

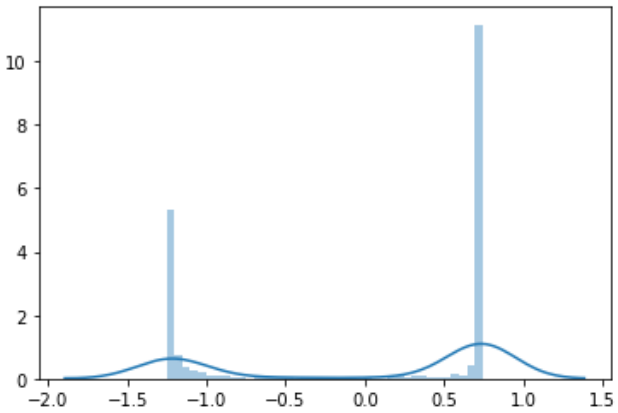

Figure 4.4: Approximated density for $\zeta = \frac{3}{2}$, $\lambda = \frac{1}{2}$ and $p = 1$

$$C_n = \begin{bmatrix} \sqrt{\frac{1}{2}} & \sqrt{\frac{1}{2}} \\ \sqrt{\frac{1}{2}} & -\sqrt{\frac{1}{2}} \end{bmatrix}$$

for all n, and we have the decoherent Hadamard walk with both coin and position spaces measurement. K. Zhang in [19] proved that the limiting distribution of the rescaled probability mass function on $\frac{\mathbb{Z}}{\sqrt{t}}$ by

$$\hat{p}(x,t) \equiv p_d(\sqrt{t}x, t), \ x \in \frac{\mathbb{Z}}{\sqrt{t}},$$

is Gaussian with mean $\mu = 0$, and variance $\sigma^2 = \frac{p + 2\sqrt{1+q^2} - 2}{p}$ where $q = 1 - p$.

Figure 4.5 shows the obtained approximated normal distribution with $\mu = 0$, and $\sigma^2 = 4\sqrt{1 + \frac{1}{4}} - 3$ generated by our algorithms.

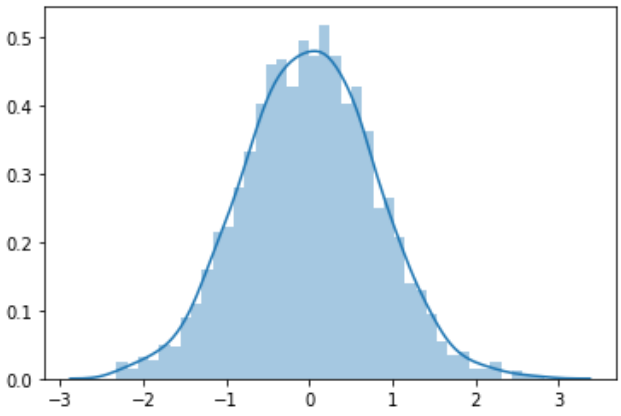

Figure 4.5: Approximated density for $\zeta = 0$, $\lambda = \frac{1}{2}$ and $p = \frac{1}{2}$

4.3.4 Estimating limiting distributions when $p < 1$

Physical intuitions tell us that whenever the pure quantum system starts being interacted by the environment, the system will become classical phenomenons in long term, in other words, the measurements can make the pure quantum system approximating the classical results. Mathematically, if the decoherent parameter p is greater than 0, the long time scaling limits should be similar to the pure classical case when $p = 1$, analogue results for decoherent analogue quantum walk were proved in [7] and [19].

First, we consider the case $\zeta = 1$. However, unlike the decoherent Hadamand walk case, for $\zeta = 1$, arcsine, uniform, and semicircle law in the interval $[-1, 1]$ have no parameters, which we can deduce that it will be difficult to find the explicit limiting distribution for $p < 1$. Thus, finding the right scaling parameter will be crucial for these cases, but we observe that if the scaling limit is n^{α}

where $\alpha \neq 1$, the densities will spread out to either infinity or accumulate to only one point. Therefore, we estimate the decoherent densities for $0 < p < 1$ with $\lambda = \frac{1}{2}, 1, \frac{3}{2}$, with the scaling exponent $\alpha = 1$.

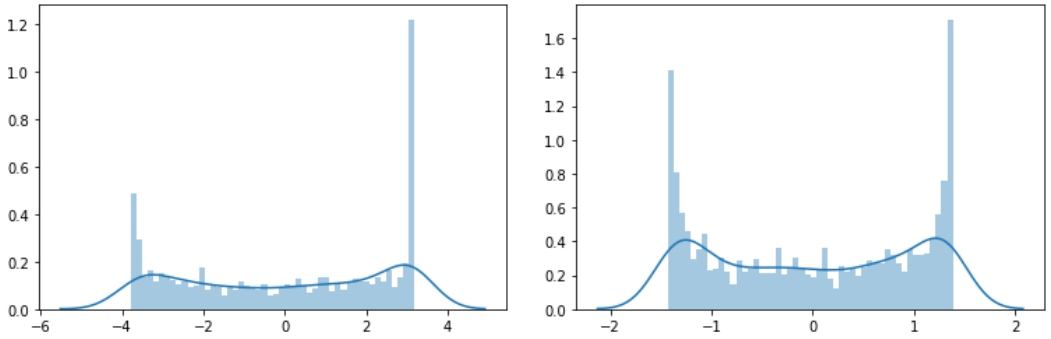

(a) $p = 0.3$ (b) $p = 0.7$

Figure 4.6: Estimated partially decoherent densities for $\zeta = 1$ and $\lambda = \frac{1}{2}$

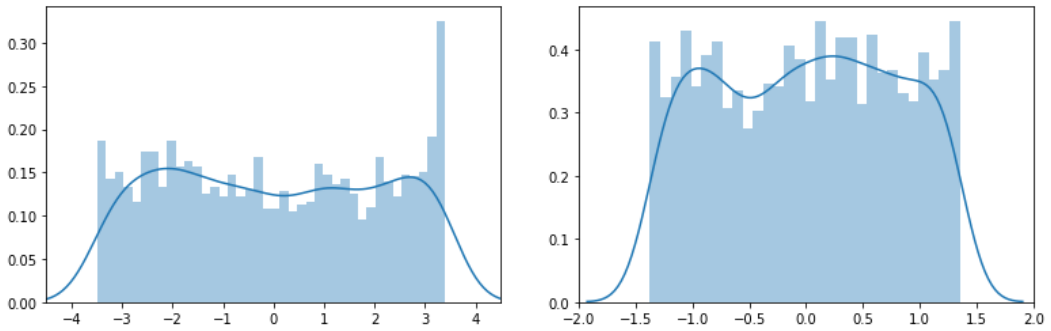

(a) $p = 0.3$ (b) $p = 0.7$

Figure 4.7: Estimated partially decoherent densities for $\zeta = 1$ and $\lambda = 1$

Figures 4.6, 4.7, and 4.8 illustrate the transitions of $\zeta = 1$ and $\lambda = \frac{1}{2}, 1, \frac{3}{2}$ (arcsine, uniform, semicircle cases respectively) when p increases. Since they

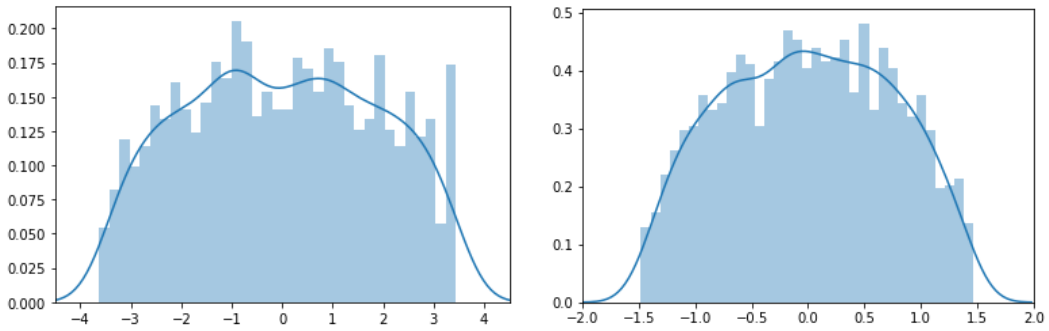

(a) $p = 0.3$ (b) $p = 0.7$

Figure 4.8: Estimated partially decoherent densities for $\zeta = 1$ and $\lambda = \frac{3}{2}$

are not parameterizable, we can only observe the transitions and compare with the classical arcsine, uniform and semicircle densities. Here, it is clear that they all have the classical distribution shapes, and when the decoherence parameter p increases, the estimated densities approximate to the classical distributions.

J. Englander and S. Volkov also proved that if $0 < \zeta < 1$, the scaling limit

$$\hat{p}(x,t) \equiv p_d(t^{\frac{(1+\zeta)}{2}}x, t), \;\; x \in \frac{\mathbb{Z}}{t^{\frac{(1+\zeta)}{2}}}$$

converges to $\mathbf{Normal}(0, \sigma^2)$ where $\sigma = \dfrac{1}{\sqrt{\lambda(1-\zeta)}}$. Which means that the limiting distribution is Gaussian with parameter σ^2 when $p = 1$. Like the homogeneous case, we expect now that the the variance of the limiting distribution may also depend on the decoherence parameter p. Even though there is no rigorous proofs about their explicit limiting distributions, we estimate the limiting distributions through our algorithm.

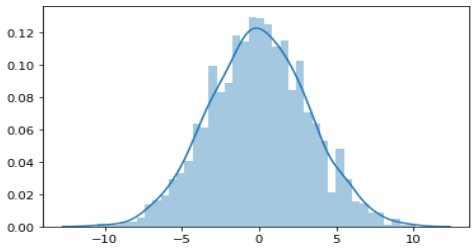

(a) $p = 0.3$

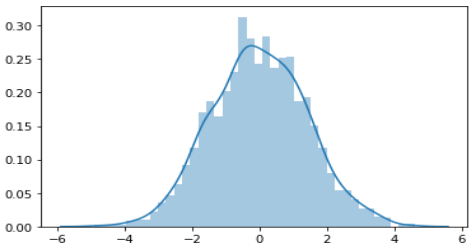

(b) $p = 0.7$

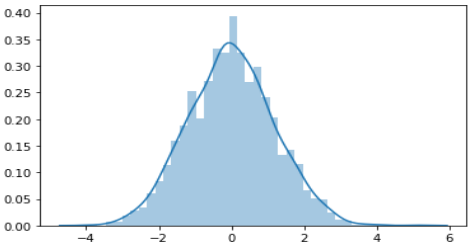

(c) $p = 1$

Figure 4.9: Estimated partially decoherent densities for $\zeta = \frac{1}{5}$ and $\lambda = \frac{1}{2}$

Figures 4.9, 4.10, and 4.11 show the simulation results for estimated densities for $\zeta = \frac{1}{5}, \frac{1}{2}, \frac{4}{5}$, and $\lambda = \frac{1}{2}$ with different p. These figures not only illustrate the transitions when p increases, but also demonstrate the normality of the densities. We can observe that for all cases, the estimated limiting distributions are Gaussian, and the variances are greater when p is small. Moreover, from Figure 4.11, we note that the convergence is slower. Therefore we can make a conjecture that the limiting distributions are normal, and the variances depend on the parameter p such that if p decreases, the variances increase.

Last case we consider is when $\lambda > 1$, and Figure 4.12 illustrate the estimated densities for $p = 0.3$ and $p = 0.7$.

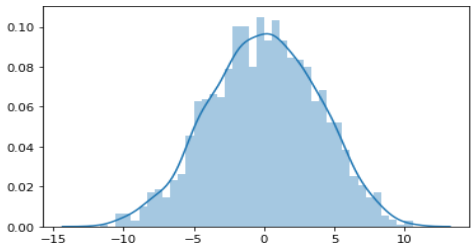

(a) $p = 0.3$

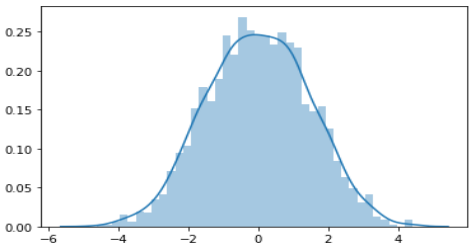

(b) $p = 0.7$

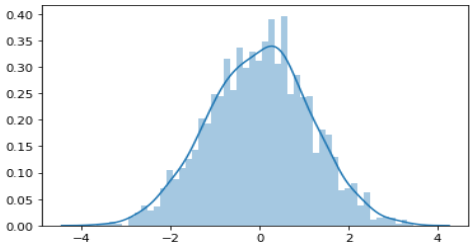

(c) $p = 1$

Figure 4.10: Estimated partially decoherent densities for $\zeta = \frac{1}{2}$ and $\lambda = \frac{1}{2}$

Note that the applications of Theorem 4.1 give us not only a analytic visualization of decoherent quantum walks in general, but also an approach to approximate classical distributions through quantum algorithms which could be useful in the future when quantum computers are fully developed.

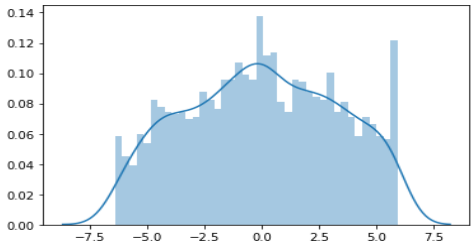

(a) $p = 0.3$

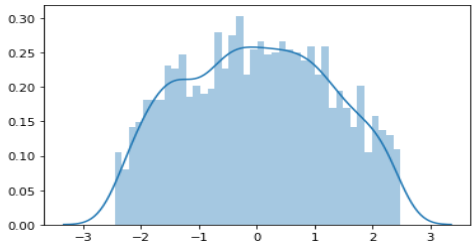

(b) $p = 0.7$

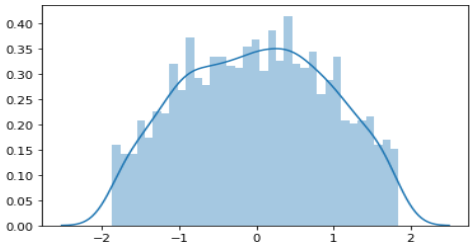

(c) $p = 1$

Figure 4.11: Estimated partially decoherent densities for $\zeta = \frac{4}{5}$ and $\lambda = \frac{1}{2}$

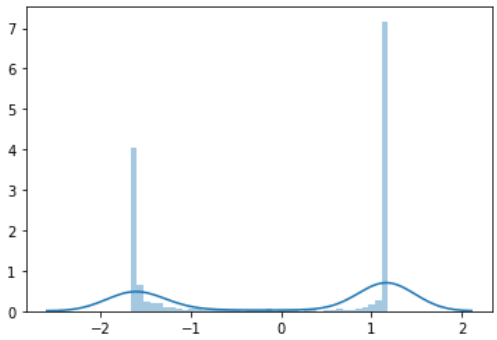

(a) $p = 0.3$

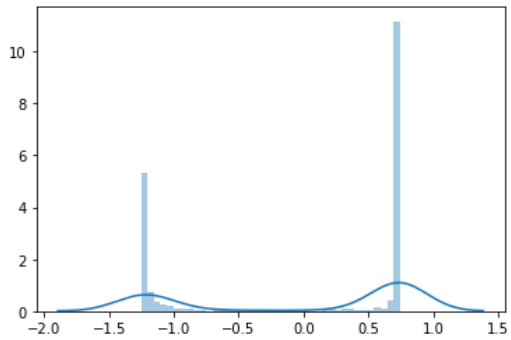

(b) $p = 7$

Figure 4.12: Estimated partially decoherent densities for $\zeta = \frac{3}{2}$ and $\lambda = \frac{1}{2}$

CHAPTER 5

QUANTIZING CLASSICAL DISTRIBUTIONS

It is time to consider the time-inhomogeneous pure quantum walk. In this case, the probability to make a measurement at each time step is $p = 0$, that means that the system maintains in the pure quantum environment. On the other hand, we know that for the complete space-time decoherent quantum walk $p = 1$ from the Chapter 4, the limiting distributions with the appropriate scaling exponents, converge to

- **Beta**(λ,λ) law when $\zeta = 1$.
- **Bernoulli**($\frac{1}{2}$) law when $\zeta > 1$.

As results, our model gives us an algorithm to determine quantum ana-

logues of these two classical distributions by taking $p = 0$ with respective parameters mentioned above. We call them quantized classical distributions. For instance, we can obtain a quantized normal distribution by considering the Hadamard Walk, and a quantized arcsine distribution by taking $p = 0$, $\zeta = 1$, and $\lambda = \frac{1}{2}$.

Unlike the decoherent quantum walk, the pure quantum walk calculation can be executed easily by linear algebra and matrices operations. Therefore, the explicit distributions can be obtained by simulation, and the quantum analogue of the classical distribution can be visualized and analyzed numerically.

5.1 Quantized Beta and Bernoulli distributions

The fact that the density of Hadamard walks, with scaling exponent 1 with symmetric initial conditions, converges to

$$\frac{1}{\pi(1+x)\sqrt{1-2x^2}} \quad \text{for} \quad x \in (-\frac{1}{\sqrt{2}}, \frac{1}{\sqrt{2}}),$$

proven by Konno in [11] (Quantized normal distribution) motivates us to study numerically the convergence of

$$\hat{p}(x,t) \equiv p_d(t^\gamma x, t), \ x \in \frac{\mathbb{Z}}{t^\gamma}, \tag{5.1}$$

with $p = 0$ and different ζ's and λ's, distributions of time-inhomogeneous pure quantum random walk. We will analyze statistically the scaling limits and the

convergence rates γ of Equation (5.1).

5.1.1 Scaling exponents for $\zeta \geq 1$

We first consider the case $\zeta \geq 1$, when the classical distributions do not converge to normal distributions. Using symmetric initial conditions,

$$\rho_0 = \frac{1}{\sqrt{2}}\big(|0\rangle \otimes |1\rangle + |0\rangle \otimes |2\rangle\big),$$

Figures 5.1, 5.2, 5.3 and 5.4 illustrate the simulation results of the quantized arcsine, uniform, semicircle , and Bernoulli law using different scaling exponents t^α with $\alpha = 0.7, 0.8, 0.9, 1$ for $t = 2000$.

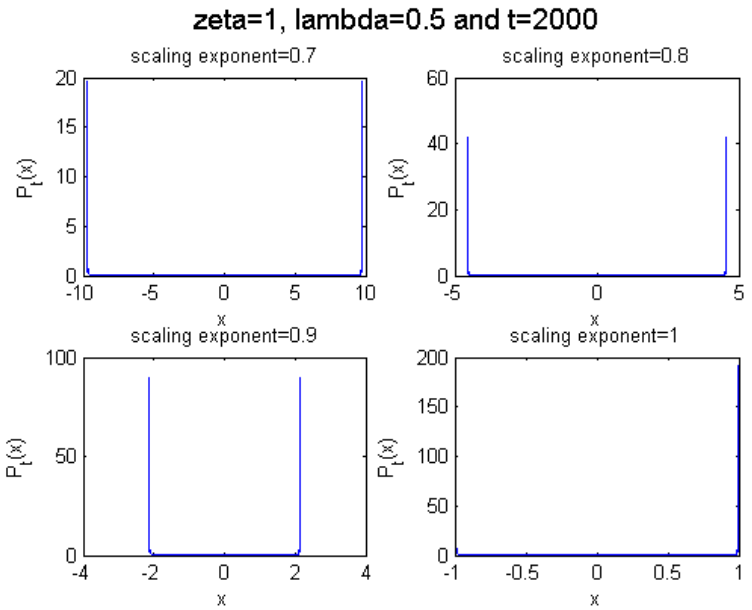

Figure 5.1: Explicit density for $\zeta = 1$, $\lambda = \frac{1}{2}$ using different scaling exponents $\alpha = 0.7, 0.8, 0.9, 1$

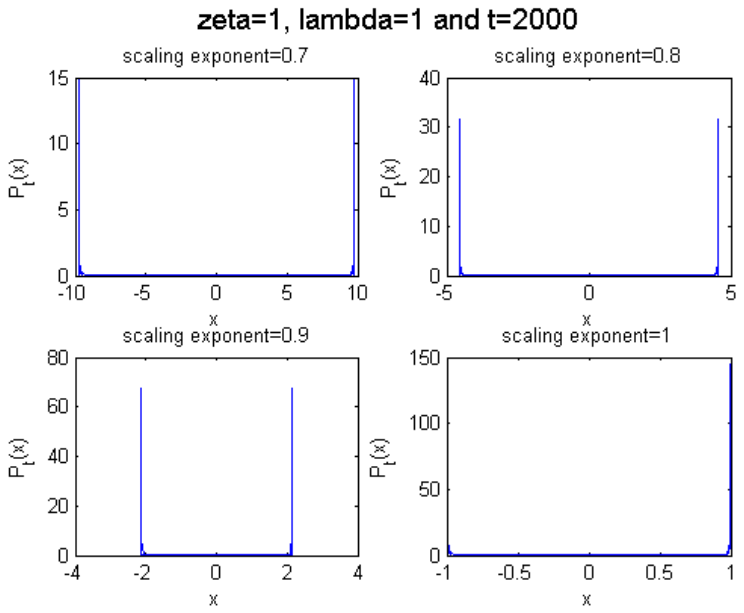

Figure 5.2: Explicit density for $\zeta = 1$, $\lambda = 1$ using different scaling exponents $\alpha = 0.7, 0.8, 0.9, 1$

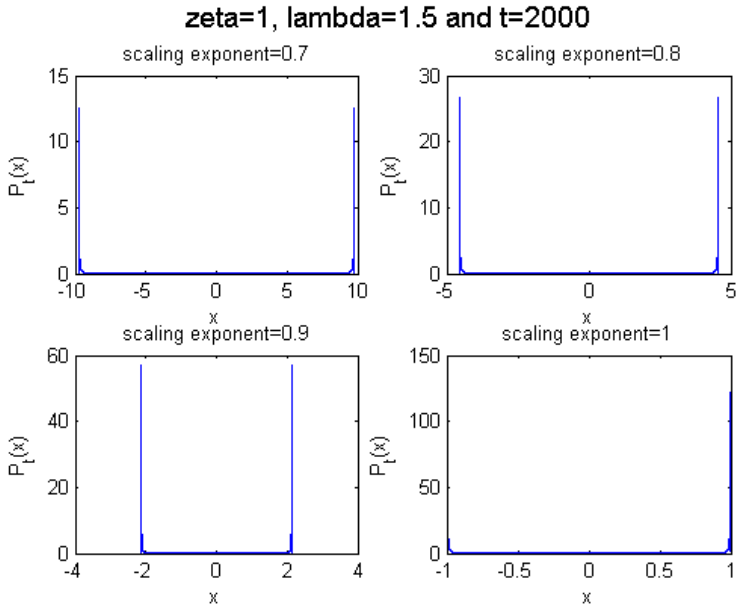

Figure 5.3: Explicit density for $\zeta = 1$, $\lambda = \frac{3}{2}$ using different scaling exponents $\alpha = 0.7, 0.8, 0.9, 1$

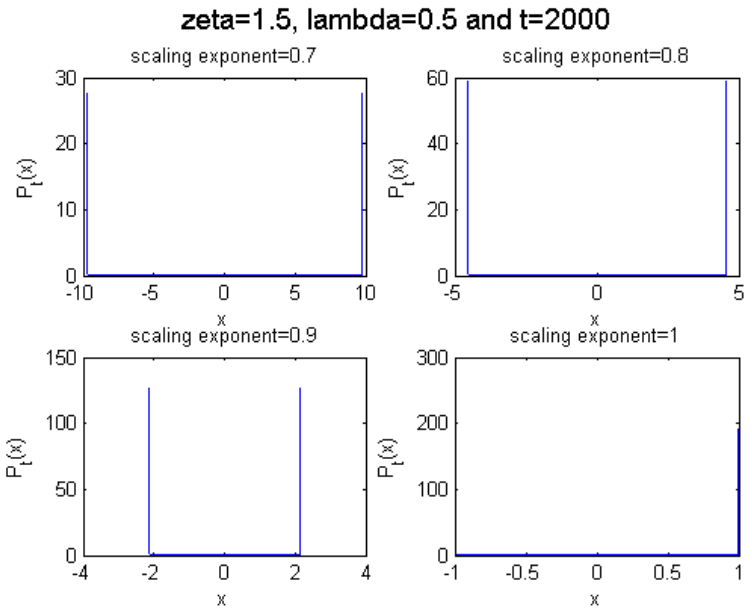

Figure 5.4: Explicit density for $\zeta = \frac{3}{2}$, $\lambda = \frac{1}{2}$ using different scaling exponents $\alpha = 0.7, 0.8, 0.9, 1$

We observe from these figures that the mass of the densities spreads rapidly to the end points of the interval. Because of the fact that $t^r \to \infty$ for $r > 0$, the mass will spread out to infinity if $\alpha < 1$, we expect that the correct scaling exponent is 1. Moreover, we also observe that even for the scaling exponent equal to 1, the mass will concentrate at the a neighborhood of the end points of the interval $[-1, 1]$. Even more, we will show numerically that the mass will concentrate at exactly two points, -1 and 1.

5.1.2 Convergent rates to Bernoulli distribution

Let's statistically analyze the convergent rates, by fixing a large t, suppose that $\alpha = 0.03$ and define

$$\epsilon_t := \min\{k \in \mathbb{N} : \sum_{i=-t}^{-t+k} p_d(i,t) \geq \frac{1-\alpha}{2}\},$$

Intuitively, since we are using symmetric initial conditions, for fix t, more than 97% of the density in the set

$$\{x \in \mathbb{Z} : x = -t, -t+1, ..., -t+\epsilon_t\} \cup \{x \in \mathbb{Z} : x = t-\epsilon_t, ..., t-1, t\},$$

In other words, ϵ_t is the length of the neighborhood from the end points $-t$ and t such that 97% of the mass is concentrated.

And now we define $\alpha_t = \frac{\epsilon_t}{t}$. Note that in this case, with fixed t, the probability that you can find the rescaled quantum walk in the interval in $[-1, -1+\alpha_t] \cup [1-\alpha_t, 1]$ is $1-\alpha$, which is,

$$\sum_{x \in [-1,-1+\alpha_t]} \hat{p}(x,t) \geq \frac{1-\alpha}{2} \quad \text{where} \quad x \in \frac{\mathbb{Z}}{t}.$$

Assuming the fact that α_t converges to 0 as $t \to \infty$, we fit two nonlinear regression: exponential decay model ce^{-rt} and rational decay model ct^{-r} in Matlab. (See [15] [10] for more details about nonlinear regression and its applications)

First, suppose that

$$\alpha_t \sim ce^{-rt},$$

taking natural logarithms both side, we obtain that

$$\ln(\alpha_t) \sim \ln(c) + (-rt).$$

Therefore, the exponential decay rate r can be obtained by

$$r = \lim_{t\to\infty} \frac{\ln(\alpha_t)}{t},$$

in other words, if t is large, r is approximately

$$r \sim \frac{\ln(\alpha_t)}{t}.$$

Second, if we assume the rational decay model $\alpha_t \sim ct^{-r}$, we can obtain by similar argument that the rational decay rate,

$$r = \lim_{t\to\infty} \frac{\ln(\alpha_t)}{\ln(t)},$$

and if t is large , $r \sim \frac{\ln(\alpha_t)}{\ln(t)}$.

Considering $t = 2000$, by taking initial vectors

$$[c_0, r_0] = [1, \frac{\ln(\alpha_{2000})}{2000}], [1, \frac{\ln(\alpha_{2000})}{\ln(2000)}]$$

for exponential and rational models respectively, we fit both models in Matlab. As results, for all three cases we considered, rational decay model has better R-squared estimate and root mean squared error (see definitions of R-squared estimate and root mean squared and Figure A.3 in Appendix A). For instance, Figures A.1(a) and A.1(b) show better results for rational decay model when $\zeta = 1$ and $\lambda = \frac{1}{2}$. The R-squared estimate of the rational decay model is

0.987, while the R-squared estimate is 0.915 for the exponential decay model. The root mean error: 0.0154 for the rational decay model and 0.0389 for the exponential decay model.

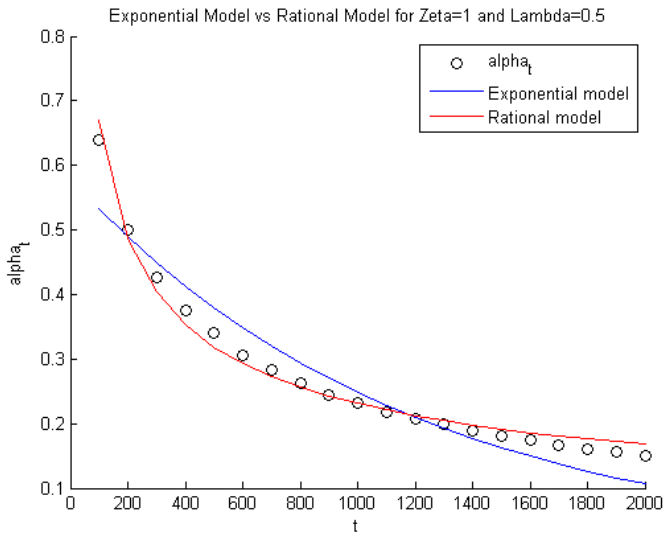

Figure 5.5: Non linear regression model comparison for $\zeta = 1$, $\lambda = \frac{1}{2}$ and $p = 0$

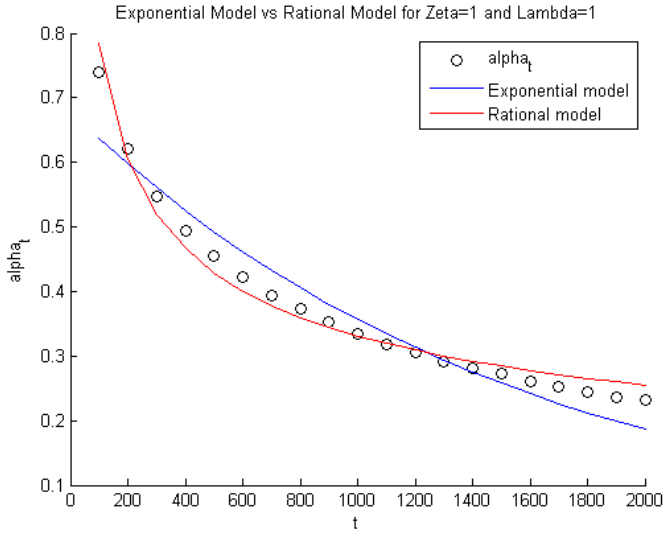

Figure 5.6: Non linear regression model comparison for $\zeta = 1$, $\lambda = 1$ and $p = 0$

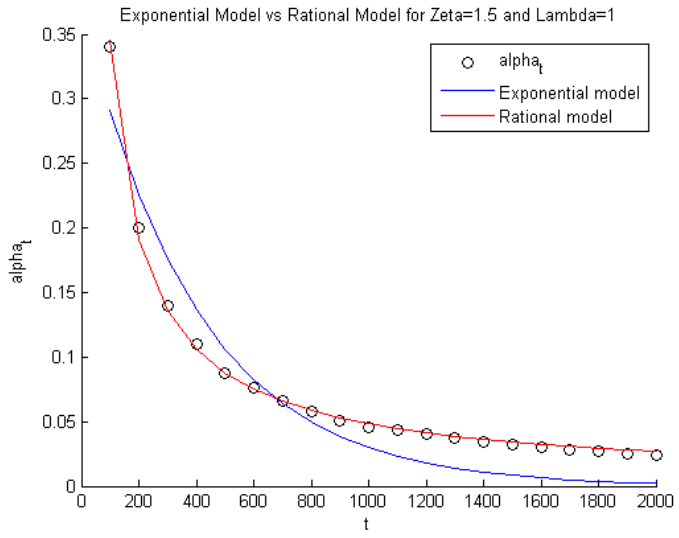

Figure 5.7: Non linear regression model comparison for $\zeta = \frac{3}{2}$, $\lambda = 1$ and $p = 0$

On the other hand, Figures 5.5, 5.6, and 5.7 show both fitted model and α_t and we observe that the rational decay model fits better . It is clear that the functions graphed by rational model using estimated coefficients by nonlinear regression behave more similarly than the functions graphed by exponential models.

Note that how fast α_t converges to 0 determines the rate of convergence to Bernoulli distribution for each ζ and λ. In order to compare numerically the rates for different values, we execute nonlinear regression for the rational model by fixing $\zeta = 1$ and varying λ. then by varying ζ and fixing $\lambda = \frac{1}{2}$. Tables 5.1 and 5.2 present estimated values of the nonlinear regression for the rational model $\alpha_t \sim ct^{-r}$ we considered.

Figures 5.8(a) and 5.8(b) illustrate the convergent rates for thse two sit-

λ	0.5	0.6	0.7	0.8	0.9	1	1.1	1.2	1.3	1.4	1.5
c	5.64	5.25	5.17	4.70	4.51	4.40	4.20	4.08	4.03	3.84	3.87
r	0.46	0.43	0.42	0.40	0.38	0.37	0.36	0.35	0.34	0.33	0.32

Table 5.1: Estimated coefficients by nonlinear regression for fixed $\zeta = 1$ and $p = 0$

ζ	1	1.1	1.2	1.3	1.4	1.5	1.6	1.7	1.8	1.9	2
c	5.64	7.23	10.67	12.11	13.86	17.48	15.47	17.46	14.28	13.96	12.06
r	0.46	0.54	0.65	0.71	0.77	0.85	0.86	0.92	0.92	0.94	0.93

Table 5.2: Estimated coefficients by nonlinear regression for fixed $\lambda = \frac{1}{2}$ and $p = 0$

uations, i.e. first fixing $\zeta = 1$ and varying λ, and then, varying ζ and fixing $\lambda = \frac{1}{2}$. Therefore, we observe from nonlinear regression results that when we fix $\zeta = 1$, the convergent rate r in function of ζ is increasing which means that the time-inhomogeneous quantum walk converges faster to Bernoulli distribution while ζ increases. On the other hand, with fixed $\lambda = \frac{1}{2}$ the convergent rate r in function of λ is decreasing which means that it converges slower to Bernoulli distribution if λ increases.

Intuitively, if $\lambda, \zeta > 0$ the transition matrix

$$C_n = \begin{bmatrix} \sqrt{1 - \frac{\lambda}{n^\zeta}} & \sqrt{\frac{\lambda}{n^\zeta}} \\ \sqrt{\frac{\lambda}{n^\zeta}} & -\sqrt{1 - \frac{\lambda}{n^\zeta}} \end{bmatrix} \to \begin{bmatrix} 1 & 0 \\ 0 & 1 \end{bmatrix},$$

and the rate the matrix converges depends on the term $\frac{\lambda}{n^\zeta}$ in the matrix. Indeed, it's clear that for large λ's and small ζ's the matrix converges slower than small λ's and large ζ's which accords to our simulation results.

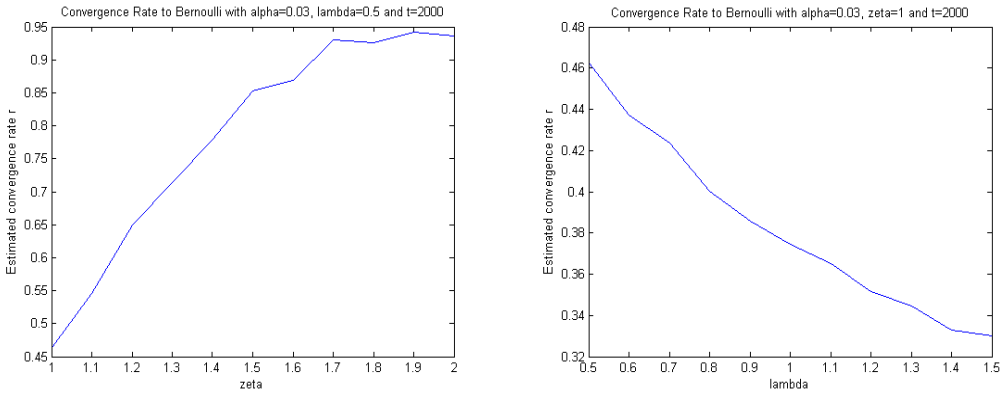

(a) $\lambda = \frac{1}{2}$ (b) $\zeta = 1$

Figure 5.8: Estimated convergence rates by rational decay model for $p = 0$

5.2 Comparison with decoherent quantum walk when $p = 1$ and $\zeta \geq 1$

After we study numerically the convergent rates of the quantum analogues of the classical distributions in the previous section, it is also interesting to compare the obtained results with the convergent rates of the decoherent walks with $p = 1$, their classical analogues. In order to do this comparison, we first fit nonlinear regression model to our model with $p = 1$ and $\zeta > 1$.

5.2.1 Convergent rates of the decoherent walk when $\zeta > 1$ to Bernoulli

Note that for $p = 1$, the densities converge to Bernoulli distribution with scaling exponent $\gamma = 1$, which says that

$$\hat{p}(x,t) \equiv p_d(tx,t),\ x \in \frac{\mathbb{Z}}{t},$$

converges to Bernoulli distribution (See [6]). Therefore, in this section, we study statistically the convergent rate of them.

Let's consider α_t as we defined in Section 5.1.2, we fit two nonlinear regression: exponential decay model ce^{-rt} and rational decay model ct^{-r} in Matlab with the same initial value formula we considered,

$$[c_0, r_0] = [1, \frac{\ln(\alpha_{2000})}{2000}], [1, \frac{\ln(\alpha_{2000})}{\ln(2000)}],$$

for exponential and rational models respectively.

As results, for all two cases we considered, rational decay model has better R-squared estimate and root mean squared error again (see Figure A.4 in Appendix A). For instance, Figures A.4(a) and A.4(b) show better results for rational decay model when $\zeta = \frac{5}{4}$ and $\lambda = \frac{1}{2}$. The R-squared estimate of the rational decay model is 0.997, while the R-squared estimate is 0.85 for the exponential decay model. The root mean error: 0.00197 for the rational decay

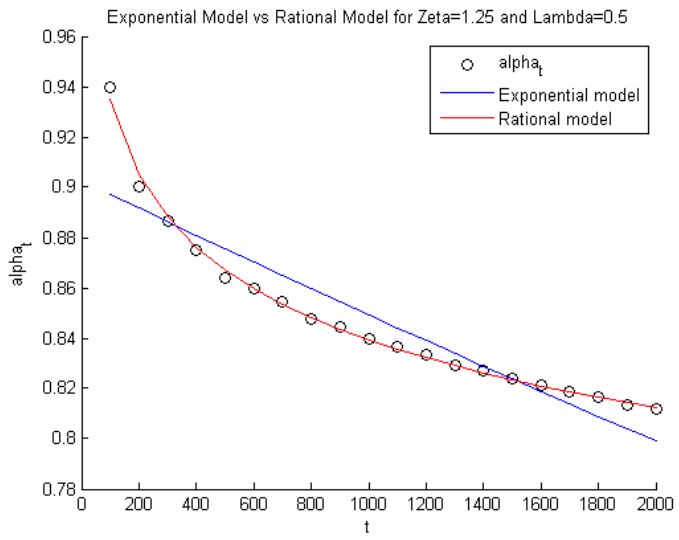

Figure 5.9: Non linear regression model comparison for $\zeta = \frac{5}{4}$, $\lambda = \frac{1}{2}$ and $p = 1$

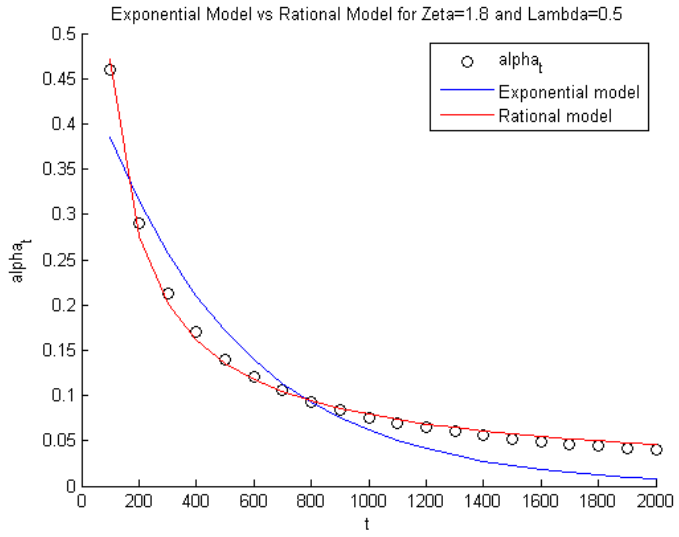

Figure 5.10: Non linear regression model comparison for $\zeta = \frac{9}{5}$, $\lambda = \frac{1}{2}$ and $p = 1$

model and 0.0131 for the exponential decay model.

Moreover, Figures 5.9 and 5.10 show both fitted model and α_t and we

observe that the rational decay model fits better . It is also clear that the functions graphed by rational model using estimated coefficients by nonlinear regression behave more similarly than the functions graphed by exponential models.

λ	0.5	0.6	0.7	0.8	0.9	1	1.1	1.2	1.3	1.4	1.5
c	3.31	2.91	2.54	2.31	2.14	1.97	1.89	1.80	1.70	1.67	1.61
r	0.30	0.26	0.22	0.20	0.18	0.16	0.15	0.14	0.13	0.12	0.11

Table 5.3: Estimated coefficients by nonlinear regression for fixed $\zeta = \frac{3}{2}$ and $p = 1$

ζ	1.25	1.35	1.45	1.55	1.65	1.75	1.85	1.95	2.05	2.15	2.25
c	1.15	1.46	2.39	4.82	8.92	14.35	18.27	18.21	19.74	13.96	10.19
r	0.05	0.10	0.22	0.39	0.56	0.71	0.82	0.89	0.96	0.94	0.93

Table 5.4: Estimated coefficients by nonlinear regression for fixed $\lambda = \frac{1}{2}$ and $p = 1$

In order to compare the convergence rates with the pure quantum case in the previous section, we execute nonlinear regression for the rational model by fixing $\zeta = \frac{3}{2}$ and varying λ. then by varying ζ and fixing $\lambda = \frac{1}{2}$. Tables 5.3 and 5.4 present estimated values of the nonlinear regression for the rational model $\alpha_t \sim ct^{-r}$ we considered.

Figures 5.11(a) and 5.11(b) illustrate the convergence rates for these two situations, i.e. first fixing $\lambda = \frac{1}{2}$ and varying ζ, and then, varying λ and fixing $\zeta = \frac{3}{2}$. Therefore, we observe from nonlinear regression results that when we fix $\zeta = \frac{3}{2}$, the convergence rate r in function of ζ is decreasing which means that the decoherent quantum walk converges faster to Bernoulli distribution

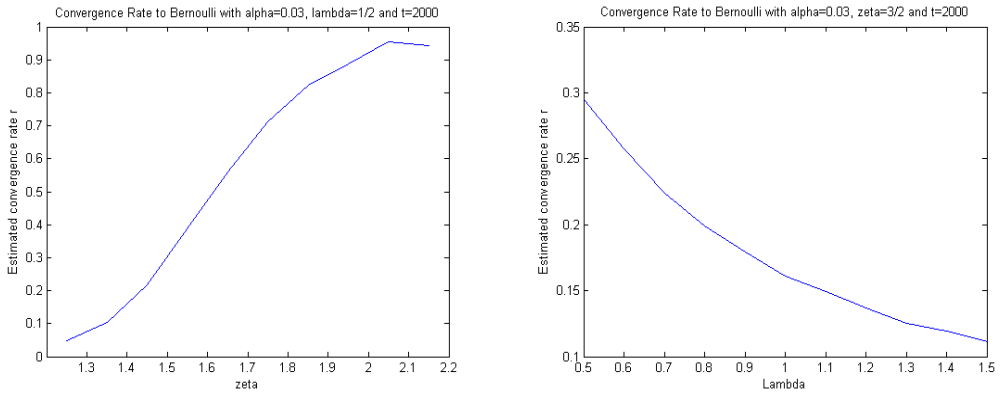

(a) $\lambda = \frac{1}{2}$ (b) $\zeta = \frac{3}{2}$

Figure 5.11: Estimated convergence rates by rational decay model for $p = 1$

while ζ increases. On the other hand, with fixed $\lambda = \frac{1}{2}$ the convergence rate r in function of λ is increasing which means that it converges slower to Bernoulli distribution if λ increases.

The most interesting thing we observe here by comparing the results from the case $p = 0$ in previous section is that not only both densities converges to Bernoulli distribution, but also the estimated convergent rates are increasing by fixing $\lambda = \frac{1}{2}$ for both $p = 0$ and $p = 1$ cases. Moreover, the ranges of estimated convergence rates for $p = 0$ and $p = 1$ are approximately $[0.45, 0.95]$ and $[0.05, 0.9]$ respectively for fixed $\lambda = \frac{1}{2}$ and $1 < \zeta < 2$, which means that the convergence to Bernoulli distribution is faster for the quantum case (see Figures 5.8(a) and 5.11(a)).

As results, our statistical analysis shows that though our model, not only

the quantum analogue of Bernoulli distribution in this case is Bernoulli distributions with the same scaling exponent, but also the convergence speed is even greater that than the decoherent walk when $p = 1$.

5.2.2 Densities of the decoherent walk when $\zeta = 1$

For this critical case, it is proven that the densities don't converge to Bernoulli distributions. Instead, they converge to symmetric Beta law with parameter λ, **Beta(λ,λ)**. (see [6])

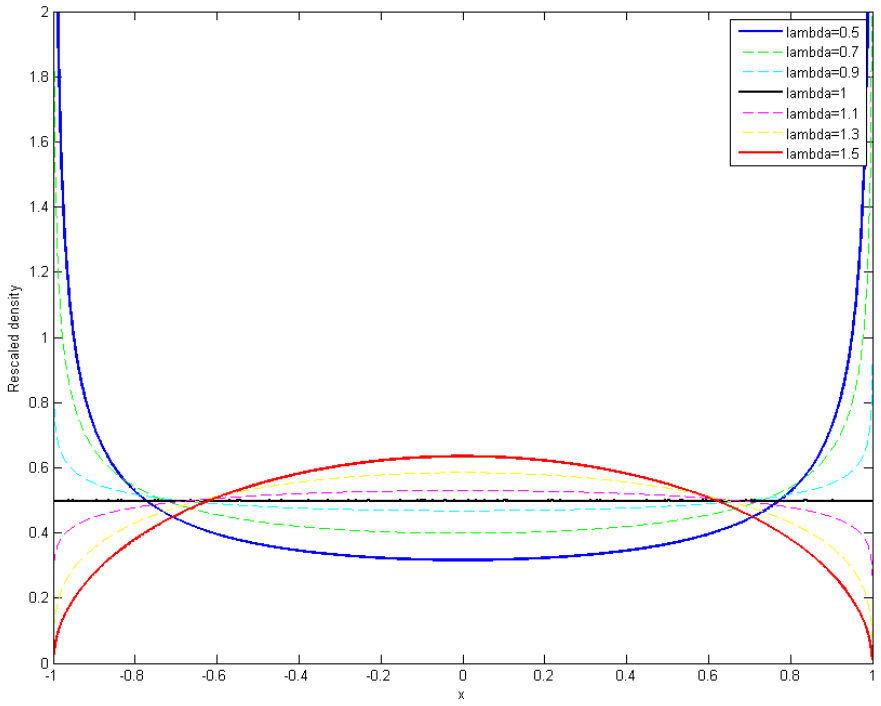

Figure 5.12: Probability densities with $t = 2000$, $\zeta = 1$ and $p = 1$

However, Figure 5.12 illustrates the densities simulated by taking $t = 2000$ with different values of λ's. We observe that when $\lambda = \frac{1}{2}, 1, \frac{3}{2}$, the figure shows approximated arcsine, uniform and semicircle densities respectively.

Therefore, this concludes statistically that even though the densities of the decoherent quantum walks for $p = 1$ converge to different classical distributions depending the values of λ, their quantum analogues converge to Bernoulli distributions with different rates of convergence showed in Section 5.1.2. Hence, the quantum analogue of the symmetric Beta distribution in this case is again Bernoulli distribution in the interval $[-1, 1]$.

CHAPTER 6

CONCLUSION

In this thesis we first considered the time-inhomogeneous unitary operators, and defined the time-inhomogeneous quantum analogue of the classical Markov chain with decoherence parameter on two dimensional finite state space and we interpreted the decoherent parameter as the probability to perform a measurement, that means that at each step, we perform a measurement with a certain probability. We proved the Markov properties at the geometric measurement times using the path integral representation, and the convergence to a equilibrium limit at large time scale when time tends to infinity.

Moreover, we generalized the result to any finite dimensional state space, and made the conclusion that the time-inhomogeneous quantum Markov chain with non zero probability of measurement also converges to an equilibrium limit as time approaches to infinity.

Second, we also defined the general time-inhomogeneous quantum walk with decoherence on the discrete infinite state space. More specifically, we studied the time-inhomogeneous quantum walk with space-coin decoherence on the set of integers with the time-inhomogeneous unitary operator using the path integral formula and its interpretation as probabilistic geometric measurement time and the time-inhomogeneous Markov chain on the coin space.

As results, we proved a representation theorem which not only gives us a better probabilistic illustration about the probability at each state, but also gives an approach to approximate the classical distribution through quantum algorithms and a tool to calculate probability densities of quantum walk with decoherence in general.

Additionally, quantized arcsine, uniform, semicircle and Bernoulli distributions were introduced by considering the time-inhomogeneous quantum walk without decoherence on the infinite discrete space. We analyzed their scaling limits and convergence rates statistically using nonlinear regression model, and concluded that not only they all converge to Bernoulli distribution with scaling exponent 1, but also the convergence speeds are higher than their classical analogues.

REFERENCES

[1] D. Aharonov, A. Ambainis, J. Kempe, and U. Vazirani. Quantum walks on graphs. *Proceedings of the thirty-third annual ACM symposium on Theory of computing*, pages 50–59, 2001.

[2] S. Broadbent and J. Hammerslfy. Percolation processes: I and II. *Cambridge Philosophical Society*, 53(1957):629–645, 1957.

[3] T. Brun, H. Carteret, and A. Ambainis. Quantum random walks with decoherent coins. *Phys. Rev.*, A 67(032304), 2003.

[4] D. Dummit and R. Foote. *Abstract Algebra, Third edition.* Wiley, 2004.

[5] R. Durrett. *Probability: theory and examples, Fifth edition.* Cambridge, 2019.

[6] J. Englander and S. Volkov. Turning a coin over instead of tossing it. *Journal of Theoretical Probability*, 31:1097–1118, 2018.

[7] S. Fan, Z. Feng, S. Xiong, and W. Yang. Convergence of quantum random walks with decoherence. *Phys. Rev.*, A 84(042317), 2011.

[8] L. Grover. A fast quantum mechanical algorithm for database search. *Proceeding of twenty-eighth annual ACM symposium Theory of computing*, pages 212–219, 1996.

[9] W. Hastings. Monte Carlo sampling methods using Markov chains and their applications. *Biometrika*, 57(1):97–109, 1970.

[10] S. Huet, A. Bouvier, M. Poursat, and E. Jolivet. *Statistical tools for nonlinear regression: a practical guide with S-PLUS and R examples.* Springer, 2004.

[11] N. Konno. A new type of limit theorems for the one-dimensional quantum random walk. *J. Math. Soc. Japan*, 57(4):1179–1195, 2005.

[12] M. Lagro and W. Yang. A Perron–Frobenius type of theorem for quantum operations. *Journal of Statistical Physics*, 169:38–62, 2017.

[13] D. Levin, Y. Peres, and E. Wilmer. *Markov Chains and Mixing Times.* AMS, 2008.

[14] N. Metropolis and S. Ulam. The Monte Carlo method. *Journal of the American statistical association*, 44(247):124–134, 1949.

[15] G. Seber and C. Wild. *Nonlinear regression.* Wiley, 2003.

[16] P. Shor. Algorithms for quantum computation: Discrete logarithms and factoring. *Foundations of Computer Science*, 1994 Proceedings 35th Annual Symposium:335–341, 1994.

[17] M. Szegedy. Quantum speed-up of Markov chain based algorithms. *Foundations of Computer Science*, Proceedings. 45th Annual IEEE Symposium:32–41, 2004.

[18] H. Zeh. On the interpretation of measurement in quantum theory. *Foundations of Physics*, 1:69–79, 1970.

[19] K. Zhang. Limiting distribution of decoherent quantum random walks. *Phys. Rev.*, A 77(062302), 2008.

APPENDIX A: NONLINEAR REGRESSION

A regression analysis is called nonlinear regression when observational data is modeled by a nonlinear predicted function of one or more independent variables (see [15] and [10] for more details). However, the following definitions of root mean square error and coefficient of determination are useful for comparing the efficiency of different fitted models.

Definition A.1 (Root mean square error) *If we have a data set of n values $y_1, ..., y_n$, each associated with a fitted value $f_1, ...f_n$, predicted values, the root mean square error is defined as*

$$RMSE = \sqrt{\frac{1}{n}\sum_{i=1}^{n}(y_i - f_i)^2}.$$

Definition A.2 (Coefficient of determination) *If we have a data set of n values $y_1, ..., y_n$, each associated with a fitted value $f_1, ...f_n$, predicted values,*

the coefficient of determination is defined as,

$$R^2 = 1 - \frac{\sum_{i=1}^{n}(y_i - f_i)^2}{\sum_{i=1}^{n}(y_i - \bar{y})^2},$$

where $\bar{y} = \frac{1}{n}\sum_{i=1}^{n} y_i$.

Definition A.3 (Adjusted coefficient of determination) *With the previous setting, adjusted coefficient of determination is defined as,*

$$\bar{R}^2 = 1 - (1 - R)^2 \frac{n-1}{n-p-1},$$

where p is the total number of explanatory variables in the model.

Simulation results

Figures in this section show the nonlinear regression results for both pure quantum walk and decoherent quantum walk cases.

Nonlinear regression model:
y ~ r1*exp(- r2*x)

Estimated Coefficients:

	Estimate	SE	tStat	pValue
r1	0.57935	0.027479	21.083	3.8669e-14
r2	0.00084697	6.5156e-05	12.999	1.3783e-10

Number of observations: 20, Error degrees of freedom: 18
Root Mean Squared Error: 0.0389
R-Squared: 0.915, Adjusted R-Squared 0.91
F-statistic vs. zero model: 580, p-value = 4.51e-17

(a) Exponential model for $\zeta = 1$ and $\lambda = \frac{1}{2}$

Nonlinear regression model:
y ~ r1*x^(- r2)

Estimated Coefficients:

	Estimate	SE	tStat	pValue
r1	5.6429	0.39236	14.382	2.6014e-11
r2	0.46259	0.011568	39.99	4.886e-19

Number of observations: 20, Error degrees of freedom: 18
Root Mean Squared Error: 0.0154
R-Squared: 0.987, Adjusted R-Squared 0.986
F-statistic vs. zero model: 3.74e+03, p-value = 2.65e-24

(b) Rational model for $\zeta = 1$ and $\lambda = \frac{1}{2}$

Figure A.1: Nonlinear regression model comparison for pure quantum walk with $\zeta = 1$, $\lambda = \frac{1}{2}$ and $t = 2000$

Nonlinear regression model:
y ~ r1*exp(- r2*x)

Estimated Coefficients:

	Estimate	SE	tStat	pValue
r1	0.68089	0.023883	28.51	1.9703e-16
r2	0.00064711	4.2471e-05	15.236	9.9189e-12

Number of observations: 20, Error degrees of freedom: 18
Root Mean Squared Error: 0.037
R-Squared: 0.933, Adjusted R-Squared 0.929
F-statistic vs. zero model: 1.13e+03, p-value = 1.18e-19

(a) Exponential model for $\zeta = 1$ and $\lambda = 1$

Nonlinear regression model:
y ~ r1*x^(- r2)

Estimated Coefficients:

	Estimate	SE	tStat	pValue
r1	4.4041	0.32746	13.449	7.8848e-11
r2	0.37473	0.012027	31.158	4.1054e-17

Number of observations: 20, Error degrees of freedom: 18
Root Mean Squared Error: 0.0211
R-Squared: 0.978, Adjusted R-Squared 0.977
F-statistic vs. zero model: 3.52e+03, p-value = 4.61e-24

(b) Rational model for $\zeta = 1$ and $\lambda = 1$

Figure A.2: Nonlinear regression model comparison for pure quantum walk with $\zeta = 1$, $\lambda = 1$ and $t = 2000$

```
Nonlinear regression model:
    y ~ r1*exp( - r2*x)

Estimated Coefficients:
         Estimate        SE        tStat       pValue
         ________    ________    ______    _________

    r1      0.37442    0.032658    11.465    1.0481e-09
    r2    0.0025284    0.0002737    9.2379    2.9813e-08

Number of observations: 20, Error degrees of freedom: 18
Root Mean Squared Error: 0.0247
R-Squared: 0.902,  Adjusted R-Squared 0.897
F-statistic vs. zero model: 175, p-value = 1.6e-12
```

(a) Exponential model for $\zeta = \frac{3}{2}$ and $\lambda = 1$

```
Nonlinear regression model:
    y ~ r1*x^( - r2)

Estimated Coefficients:
         Estimate        SE        tStat       pValue
         ________    ________    ______    _________

    r1      17.481     0.81571     21.43    2.9133e-14
    r2     0.85219    0.0087906    96.942    6.3298e-26

Number of observations: 20, Error degrees of freedom: 18
Root Mean Squared Error: 0.00342
R-Squared: 0.998,  Adjusted R-Squared 0.998
F-statistic vs. zero model: 9.55e+03, p-value = 5.79e-28
```

(b) Rational model for $\zeta = \frac{3}{2}$ and $\lambda = 1$

Figure A.3: Nonlinear regression model comparison for pure quantum walk with $\zeta = \frac{3}{2}$, $\lambda = 1$ and $t = 2000$

```
Nonlinear regression model:
    y ~ r1*exp( - r2*x)

Estimated Coefficients:
         Estimate        SE        tStat       pValue
         ________    ________    ______    _________

    r1      0.90265    0.0063037    143.19    5.6995e-29
    r2    6.0947e-05    6.0091e-06    10.142    7.1804e-09

Number of observations: 20, Error degrees of freedom: 18
Root Mean Squared Error: 0.0131
R-Squared: 0.85,  Adjusted R-Squared 0.842
F-statistic vs. zero model: 4.18e+04, p-value = 9.99e-34
```

(a) Exponential model for $\zeta = \frac{5}{4}$ and $\lambda = \frac{1}{2}$

```
Nonlinear regression model:
    y ~ r1*x^( - r2)

Estimated Coefficients:
         Estimate        SE        tStat       pValue
         ________    ________    ______    _________

    r1      1.1598    0.0049139    236.01    7.1065e-33
    r2    0.046817    0.0006313    74.159    7.7738e-24

Number of observations: 20, Error degrees of freedom: 18
Root Mean Squared Error: 0.00197
R-Squared: 0.997,  Adjusted R-Squared 0.996
F-statistic vs. zero model: 1.84e+06, p-value = 1.57e-48
```

(b) Rational model for $\zeta = \frac{5}{4}$ and $\lambda = \frac{1}{2}$

Figure A.4: Nonlinear regression model comparison for decoherent quantum walk with $\zeta = \frac{5}{4}$, $\lambda = \frac{1}{2}$ and $t = 2000$

Nonlinear regression model:
y ~ r1*exp(- r2*x)

Estimated Coefficients:

	Estimate	SE	tStat	pValue
r1	0.47258	0.037077	12.746	1.9005e-10
r2	0.0020314	0.00020399	9.9583	9.524e-09

Number of observations: 20, Error degrees of freedom: 18
Root Mean Squared Error: 0.033
R-Squared: 0.905, Adjusted R-Squared 0.9
F-statistic vs. zero model: 205, p-value = 4.09e-13

(a) Exponential model for $\zeta = \frac{9}{5}$ and $\lambda = \frac{1}{2}$

Nonlinear regression model:
y ~ r1*x^(- r2)

Estimated Coefficients:

	Estimate	SE	tStat	pValue
r1	16.789	1.0888	15.42	8.1153e-12
r2	0.77572	0.011952	64.903	8.4947e-23

Number of observations: 20, Error degrees of freedom: 18
Root Mean Squared Error: 0.00714
R-Squared: 0.996, Adjusted R-Squared 0.995
F-statistic vs. zero model: 4.55e+03, p-value = 4.55e-25

(b) Rational model for $\zeta = \frac{9}{5}$ and $\lambda = \frac{1}{2}$

Figure A.5: Nonlinear regression model comparison for decoherent quantum walk with $\zeta = \frac{9}{5}$, $\lambda = \frac{1}{2}$ and $t = 2000$

APPENDIX B: PYTHON CODE

Geometric times

The function "generateGeometricTimes" generates a sequence of geometric distribution numbers, and returns the sum of those numbers, see Figure B.1.

```
def generateGemetricTimes(t,p):
    # this function generate a sequance of geometric distribution numbers and
    # then take the sum of those numbers

    tempVector=random.geometric(p,t);
    vector = np.zeros(t+1,dtype=int);
    vector[1]=tempVector[0];
    i=1;
    while vector[i]<t:
        vector[i+1]=tempVector[i]+vector[i];
        i += 1
    vector[i]=t;
    return vector[0:i+1]
```

Figure B.1: Generation of numbers with geometric distribution

Time-inhomogeneous unitary operator

The function "generateMatrixU" returns the unitary matrix

$$U_n = \begin{bmatrix} \sqrt{1-\frac{\lambda}{n^\zeta}} & \sqrt{\frac{\lambda}{n^\zeta}} \\ \sqrt{\frac{\lambda}{n^\zeta}} & -\sqrt{1-\frac{\lambda}{n^\zeta}} \end{bmatrix},$$

see Figure B.2.

```
def generateMatrixU(n,zeta,lmda):
    #This function generate the unitary matrix U with the respect parameters
    matrix=np.array([[math.sqrt(1-(lmda/(n**zeta))), math.sqrt(lmda/(n**zeta))]
           [math.sqrt(lmda/(n**zeta)), -math.sqrt(1-(lmda/(n**zeta)))]]);
    return matrix;
```

Figure B.2: Generation of the time-inhomogeneous unitary operator U

Time-inhomogeneous Markov matrix Q

The function "generateMatrizQ" generates the matrix Q defined in Definition 3.1.

```
def generateMatrixQ(n,m,zeta,lmda):
    #This function generates the each Q with repect to n and m
    productQ = np.array([[1,0],
                         [0,1]]);

    for i in range(n+1,m+1):
        #matrix = generateMatrixU(i,zeta,lmda);
        productQ = np.dot(generateMatrixU(i,zeta,lmda),productQ);

    productQ=productQ**2;
    return productQ;
```

Figure B.3: Generation of the time-inhomogeneous Markov matrix Q

Evolution operator for discrete infinite space

The function "EvolutionOp" applies the evolution operator defined in Definition 2.4 using standard shift with unitary matrix U.

```
def EvolutionOp(state,U):
    #This function generate the simple evolution from any pure state,
    #will return two vectors
    resultStates = np.zeros((3,2));


    resultStates[:,0]= state[:];
    resultStates[1,0]= state[1]+1;

    resultStates[:,1]= state[:];
    resultStates[1,1]= state[1]-1;

    if state[2]==1:
        resultStates[0,0]= state[0]*U[0,0];
        resultStates[0,1]= state[0]*U[1,0];
        resultStates[2,1]=2;
    else:
        resultStates[0,0]= state[0]*U[1,0];
        resultStates[2,0]=1;
        resultStates[0,1]= state[0]*U[1,1];
        resultStates[2,1]=2;
    return resultStates
```

Figure B.4: Evolution operator for quantum walks

Markov chain I

The function "generateMarkovI" generates the Markov chain I defined in the proof of Theorem 4.1.

```
def generateMarkovI(I,markovR,numSampleI):
    #This function generate the corresponding I using the Markove transition
    tempI = np.zeros((1,numSampleI));
    for k in range(numSampleI):
        if I[0,k]==1:
            randomI = rv_discrete(values=(range(1,3), markovR[0,:]));
            tempI[0,k] = randomI.rvs(size=1);
        else:
            randomI = rv_discrete(values=(range(1,3), markovR[1,:]));
            tempI[0,k] = randomI.rvs(size=1);

    return tempI
```

Figure B.5: Evolution of the Markov chain I